AD-A177 094 WAKE INTERACTION EFFECTS ON THE TRANSITION PROCESS ON TURBINE BLADES(U) OXFORD UNIV (ENGLAND) DEPT OF ENGINEERING SCIENCE 30 OCT 86 AFOSR-TR-87-0100 1/1

UNCLASSIFIED AFOSR-85-0295 F/G 20/4 NL

END
DATE
FILMED
2 87

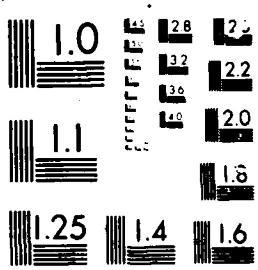
1.0
2.8
3.2
2.2
3.6
4.0
2.0
1.1
1.8
1.25
1.4
1.6

AD-A177 094

UNCLASSIFIED

SECURITY CLASSIFICATION OF THIS PAGE (2)

REPORT DOCUMENTATION PAGE

DTIC ELECTE FEB 2 4 1987 S D D

1a. REPORT SECURITY CLASSIFICATION: UNCLASSIFIED	1b. RESTRICTIVE MARKINGS
2a. SECURITY CLASSIFICATION AUTHORITY	3. DISTRIBUTION/AVAILABILITY OF REPORT: Approved for Public Release; Distribution Unlimited
2b. DECLASSIFICATION / DOWNGRADING SCHEDULE	
4. PERFORMING ORGANIZATION REPORT NUMBER(S)	5. MONITORING ORGANIZATION REPORT NUMBER(S): AFOSR-TR- 87-0108
6a. NAME OF PERFORMING ORGANIZATION: Oxford University	6b. OFFICE SYMBOL (If applicable)
7a. NAME OF MONITORING ORGANIZATION: European Office of Aerospace Research and Development/LTV	
6c. ADDRESS (City, State, and ZIP Code): Department of Engineering Science, Parks Road, Oxford, OX1 3PJ, England	7b. ADDRESS (City, State, and ZIP Code): Box 14, FPO New York 09510-0200
8a. NAME OF FUNDING/SPONSORING ORGANIZATION: Air Force Office of Scientific Research	8b. OFFICE SYMBOL (If applicable): NA
9. PROCUREMENT INSTRUMENT IDENTIFICATION NUMBER: AFOSR 85-0295	
8c. ADDRESS (City, State, and ZIP Code): Bolling AFB, DC 20332-6448 Bldg 410	10. SOURCE OF FUNDING NUMBERS

PROGRAM ELEMENT NO	PROJECT NO	TASK NO.	WORK UNIT ACCESSION NO.
61102F	2307	A4	

11. TITLE (Include Security Classification): WAKE INTERACTION EFFECTS ON THE TRANSITION PROCESS ON TURBINE BLADES

12. PERSONAL AUTHOR(S): D. L. Schultz and J. E. LaGraff

13a. TYPE OF REPORT	13b. TIME COVERED	14. DATE OF REPORT (Year, Month, Day)	15. PAGE COUNT
Annual Scientific	FROM 1 Sep 85 TO 31Aug86	1986 October 30	17

16. SUPPLEMENTARY NOTATION

17. COSATI CODES			18. SUBJECT TERMS (Continue on reverse if necessary and identify by block number)
FIELD	GROUP	SUB-GROUP	Gas Turbine Heat Transfer, Unsteady Wake Interactions, Boundary Layer Transition.

19. ABSTRACT (Continue on reverse if necessary and identify by block number)

Wide bandwidth (100 kHz) heat transfer instrumentation was used to make detailed time resolved measurements on a 2-D gas turbine rotor cascade blade surface under the influence of simulated unsteady wake and shock passing events. The instrumentation was capable of detecting and tracking naturally occurring transitional turbulent spots confirming the classical model of boundary layer transition. In addition instantaneous large excursions in the surface heat transfer were observed as the simulated wake and shock structure from a transonic nozzle guide wave passed over the rotor cascade. The transitional behavior of the blade boundary layer was seen to depend primarily on free stream turbulence and Reynolds number and, away from the direct interaction region, to be relatively unaffected by the wake/shock induced disturbances.

20. DISTRIBUTION/AVAILABILITY OF ABSTRACT: ☒ UNCLASSIFIED/UNLIMITED ☐ SAME AS RPT ☐ DTIC USERS	21. ABSTRACT SECURITY CLASSIFICATION: UNCLASSIFIED
22a. NAME OF RESPONSIBLE INDIVIDUAL: Dr. James D. Wilson, AFOSR	22b. TELEPHONE (Include Area Code): (202) 767-4987 — 22c. OFFICE SYMBOL: NA

DD FORM 1473, 84 MAR — 83 APR edition may be used until exhausted. All other editions are obsolete.

SECURITY CLASSIFICATION OF THIS PAGE

DTIC FILE COPY

AFOSR-TR- 87-0108

Grant Number: AFOSR-85-0295

WAKE INTERACTION EFFECTS ON THE TRANSITION PROCESS ON TURBINE BLADES

D.L. Schultz
Dept. of Engineering Science
Oxford University
Oxford, England

J.E. LaGraff
Dept. of Mechanical and
Aerospace Engineering
Syracuse University
Syracuse, NY, USA, 13244

30 Oct. 1986

Scientific Report No. 1

Approved for Public Release;
distribution unlimited.

Prepared for:
United States Air Force
Air Force Office of Scientific Research
Building 410
Bolling AFB, D.C. 20332
and
European Office of Aerospace Research and Development
London, England

Table of Contents

Preface

The Department of Engineering Science at Oxford University, Oxford, U.K., has had an active turbomachinery research group for over 15 years. Major contributions to the literature of fundamental measurements in turbine blade heat transfer are well established worldwide. Professor LaGraff has closely followed the contributions of the Oxford group for many years, taking a sabbatical leave at Oxford from Syracuse University for seven months in 1983. The research conducted during this visit lead directly to a proposal for a follow-on experimental program , viz., examining in some detail the transitional behavior of the boundary layer under the influence of wake/shock induced unsteadiness. Preparation for this work began in the summer of 1985, with travel support from the National Science Foundation (Grant No. INT-8509407). The first stage of the work reported herein was completed in the summer of 1986. Prof. LaGraff was on-site from May to August 1986 when access to the primary test facility was scheduled. Brief visits before and after the primary test times were also made in October 1985, March 1986, September 1986, and October 1986.

I. Introduction

A new type of transient cascade has been developed at Oxford University which has substantially improved knowledge of the distribution of heat transfer rates over turbine bladings. This facility, described briefly below, allows the testing of actual blade profiles at full scale engine Reynolds numbers, Mach numbers and gas-to-wall temperature ratios. The theory of operation and typical results are discussed in detail in References 1 and 2. A summary of the facility and instrumentation are included in the next two parts of this report for completeness. (See e.g. Fig. 1).

Of special interest in comparing cascade tests with real engine rigs is to account for the flow unsteadiness associated with wake-passing phenomena between adjacent stages. Some recent work has been reported which has begun to unravel this complex flow field in a systematic manner (see e.g. Refs. 3 and 4). Very recently Doorly (Ref. 5) has reported detailed time-resolved heat transfer and aerodynamic measurements of a wake passing experiment in the Oxford cascade. In this experiment the wakes were generated by a rotating set of cylindrical wires upstream of the stationary rotor cascade (Fig.2). Significant changes in the cascade flow and heat transfer rates were observed during each wake passing event. Subsequent work in the Oxford cascade on a new blade profile was systematically undertaken at various Mach numbers, Reynolds numbers and blade incident angles to determine the wake passing vs. no wake results (Ref. 6) with the intention of ultimately comparing this with tests on the same blade on the new MIT Gas Turbine Laboratory transient, rotating, blow- down rig. These comparisons are not complete at this date.

II. The Experimental Technique

a) Isentropic Light Piston Tunnel Cascade

Transient techniques have long been recognized as a powerful technique for heat transfer measurements. (Ref. 7.). Short duration shock heated facilities had particular success simulating the high enthalpy environment characteristic of hypersonic reentry conditions from orbital and suborbital flight. Inferring instantaneous heat transfer rates from the transient response of the surface temperature of models (see next section) greatly eased the instrumentation problems in the high temperature environment of steady state facilities, and substantially reduced the operating costs compared to long duration testing.

In recent years (Refs. 8,9,10) transient facilities have found application at the more modest enthalpy levels, but experimentally awkward environment, of gas turbine engines (transonic, rotating, $R_e = 10^6$ +, $T_0/T_w = 1.5 \rightarrow 2.0$). A particularly productive approach has been the one developed at Oxford University (Ref. 1) where shock heating has been replaced by a piston driven isentropic compression process. A fundamental advantage of this approach is that the running time is increased by one or two orders of magnitude over the shock heated mode while still offering the advantages of transient techniques. The increased running time offers significant instrumentation advantages not possible in shock heated facilities, including 1) greater ease of simultaneous direct digital sampling of multichannel instrumentation, 2) the possibility of multichannel surface pressure measurements through relatively long lengths of tubing to transducers mounted external to the small models, 3) surface oil drop flow visualization and, 4) airfoil wake pressure traverses yielding the loss measurements which are of

significant interest to turbine aerodynamicists. Light piston isentropic compression tunnels, while now well established at two centers in Europe (Oxford and Von Karman Institute), have not received much attention in the USA. A comprehensive discussion of the theory of the light piston facility can be found in Reference 2. Basically the running time of the piston facility is limited by the driven tube volume and not its length as in a shock tube. Thus, short length but large diameter tubes can sustain a large mass flow even through the relatively large throat areas of five-blade cascade rows and not be limited by the wave reflection process that dominates shock tunnels. As a result, exceptionally steady flow rates for up to 0.5 seconds are easily achieved in the light piston facility. The Oxford facility is routinely operated at full scale engine Reynolds number and Mach number and at gas to metal (wall) temperature ratios of 1.5 or higher, simulating the important parameters for turbine blade aerodynamics and heat transfer. Equally important is the fact that these parameters can be varied independently. A brief discussion of the heat transfer instrumentation for the reported work follows in the next section.

b) *Instrumentation*

The instrumentation central to the reported research involves the high bandwidth heat transfer measurements. The sensors are thin film resistance thermometers fired onto a blade profile which has been machined out of a glass ceramic. The surface temperature is monitored and easily converted to an instantaneous heat transfer rate using as a signal processor an electrical analogue of the 1-D heat conduction equation. Figure 3 shows an example of an instrumentated blade, the signal processing, and typical results for heat transfer and surface

temperature response. For convenient comparisons, it is usual to extrapolate instantaneous heat transfer rates for various points on the blade to a uniform (isothermal) initial surface temperature. Such an extrapolation procedure is also shown in Figure 3.

Special electronics have been reported by Oldfield et.al. (Reference 11) which raise the effective bandwidth of the instrumentation package to 100 KHz, sufficient for observing individual wake-passing events. Figure 4 shows typical results for surface heat transfer from Reference 6. The high time resolution data were recorded on two 8 channel Datalab Model DL2800 Transient Recorders where 4096 point were recorded on each channel at a rate of up to 2 MHz/channel.

III. Research Proposed on Boundary Layer Transition with Wake Interactions

Recently studies have been made of the effect of the unsteady flows caused by nozzle-wake/rotor blade interactions. (Refs. 5 and 6). These studies have shown that several effects occur in an interactive manner and include boundary layer disturbances due to incidence changes, shock impingement (from the NGV wake) and early transition caused by the increase in free stream turbulence as the wake from the NGV's passes through the turbine passage. In previous work, tracking of the boundary layer transition has been done with the span-wise thin film transducers approximately 10mm wide which 'average' the heat transfer rate spanwise. The transducers themselves have a very wide bandwidth 0.1 Hz → 100 kHz and so can resolve the rapid phenomena associated with conventional "turbulent spot" growth, (Refs. 12,13,14). What was proposed was to determine whether the process of transition on a turbine blade resembles that on a stationary aerofoils. The technique developed at Oxford produces a

relative motion between a rotor and nozzle guide vane by means of a rotating set of bars (20-25000 RPM) upstream of the rotor. (Fig. 2). The wake is designed to be correct in magnitude of momentum deficit and dimensions to replicate that of the NGV. The rotor is stationary. High speed heat transfer gauges on the rotor are used to determine the blade-wake interaction and are capable of tracking the conjectured transition 'spots'.

The proposed first year study was a basic analysis of the transition process on 2-D cascade airfoil under the influence of simulated wakes passing over the surface. The methodology involved wide bandwidth heat transfer instrumentation (closely spaced narrow thin film thermometers) and high speed digital data recorders allowing up to 16 channels of simultaneous time-resolved data. With this data, correlation spectra could be extracted while tracking transitional events in the blade boundary layer.

IV. Summary of Results

A fully documented scientific summary of the results of the first year of the program are contained in Ref. 16 (a copy is attached in Appendix A). This paper has been accepted at the Japanese Society of Mechanical Engineers/American Society of Mechanical Engineers 2nd Joint Thermal Engineering Conference scheduled for March 1987. A brief summary (Ref. 17) of the work was submitted as part of a more comprehensive paper submitted to the AGARD Propulsion and Energetics Panel Meeting in Neubiberg, W. Germany in September 1986 (A copy of this paper is attached in Appendix B).

The results verified first of all the experimental approach. Narrow,

closely spaced, thin film constant current surface thermometers coupled with wide bandwidth electrical analogue circuits and high-speed-multi-channel digital data acquisition could detect and precisely track transient aerodynamic events on the 2-D turbine blade surface. Specifically, discrete turbulent spot events were seen to appear in the laminar boundary layer heat transfer traces, to grown and finally merge (in the high Reynolds number case) giving a "steady" turbulent heat transfer level. The heat transfer traces between the turbulent spots returned precisely to the levels of the laminar values (obtained over the entire blade with low free stream turbulence). The detail of the transitional signals allowed individual spots to be identified and followed from film to film. Correlation spectra showed very high correlation coefficients between channels over a time span which included, multiple turbulent spot events. Quantification of the state of the boundary layer was easily achieved using a standard intermmittency definition.

After quantifying the state of the individual boundary layer (for both the laminar case and natural transition case), the tests proceeded to investigate the influence of the wake-passing events with and without the shock waves which would occur on a transonic stage. Although the behavior was quite complex the basic results indicated that the region between the wake-passing events behaved in much the same way as the natural (undisturbed) boundary layer over the entire blade. Coincident with the wake and shock disturbances, however, were unsteady excursions in the heat transfer which were very marked near the front of the blade (including apparent separation of the boundary layer as the shock swept by) and continuing as an enharced heat

transfer along the blade surface as far as the instrumentation covered.

Preparations are underway for the extension of the present studies to a fully annular rotating transonic stage. This work will enter the test phase in the summer of 1987.

References

1. Schultz, D.L., T.V. Jones and M.L.G. Oldfield, *A New Transient Cascade Facility for the Measurement of Heat Transfer Rates,* AGARD CP-229, 1977.

2. Schultz, D.L., M.L.G. Oldfield and T.V. Jones, *Heat Transfer Rate and Film Cooling Effectiveness Measurements in a Transient Cascade,* AGARD CP-281, 1980.

3. Dring, R.P., H.D. Joslyn, L.W. Hardin and J.H. Wagner, *Turbine Rotor-Stator Interactions,* ASME Gas Turbine Division 82-GT-3, April 1982.

4. Dunn, M.G. and A. Hause, *Measurments of Heat Flux and Pressure in a Turbine Stage,* J. Eng. for Power, Vol. 104, Jan. 1982.

5. Doorly, D.J., M.L.G. Oldfield and C.T.J. Scrivener, *Wake Passing in a Turbine Rotor Cascade,* AGARD Propulsion and Energetics Panel 65th Symposium, May 1985, Bergen, Norway.

6. Ashworth, D.A., J.E. LaGraff, D.L. Schultz, and K.J. Grindrod, *Unsteady Aerodynamic and Heat Transfer Processes in a Transonic Turbine Stage,* J. Eng. for Gas Turb. and Power, Vol. 107, Oct. 1985.

7. Holder, D.W. and D.L. Schultz, *On the Flow in a Reflected Shock Tunnel,* Aero. Res. Council (UK) R & M 3265, 1962.

8. Jones, T.V. and D.L. Schultz, *A Study of Film Cooling Related to Gas Turbines Using Transient Techniques,* Aero. Res. Council (UK) ARC 32420, HMT 261, 1970.

9. Louis, J.F. A.M. Demergian, G.N. Goulios, and R.F. Topping, *Short Duration Studies of Turbine Heat Transfer and Film Cooling Effectiveness,* ASME-GT-131, 1974,

10. Dunn, M.F. and F.J. Stoddard, *Application of Shock Tube Technology to the Measurement of Heat-Transfer Rate to Gas Turbine Components,* Proceedings of the Eleventh International Symposium on Shock Tubes and Waves, University of Washington Press, (Editors B. Ahlbard, A. Hertzberg, D. Russell), 1978.

11. Oldfield, M.L.G., H.J. Burd and N.G. Doe, *Design of Wide-Bandwidth Analogue Circuits for Heat Transfer Instrumentation in Transient Tunnels,* Proceedings of 16th Symposium of the International Center for Heat and Mass Transfer, Dubrovnik, 1982, Hemisphere Publishing Corp. (1984), (Metzger and Afgan, Editors).

12. Oldfield, M.L.G., R. Kiock, A.T. Holmes, and C.G. Graham, *Boundary Layer Studies on Highly Loaded Cascades Using Thin Films and a Traversing Probe,* J. of Engineering for Power, Vol. 103, No. 1, 1981.

13 LaGraff, J.E., *Observation of Boundary Layer Transition in a Mach 7 Gun Tunnel with a Hot Wire Anemometer,* AIAA Journal, Vol. 10, No. 6, 1972.

14. Nicholson, J.H., *D. Phil. Thesis,* Oxford University, 1981.

15. Doorly, D.J. and Oldfield, M.L.G., *Simulation of the Effects of Shock Wave Passing on a Turbine Rotor Blade,* J. Engr. for Gas and Turbine Power, Vol. 107, October, 1985.

16. Ashworth, D.A., LaGraff, J.E. and Schultz, D.L., *Unsteady Interaction Effects on a Transitional Turbine Blade Boundary Layer,* to be presented, 2nd Joint JSME/ASME Thermal Engineering Conference, Honolulu, March 1987.

17. Schultz, D.L., Ashworth, D.A., LaGraff, J.E., Johnson, A.B. and Rigby, M.L., *Wake and Shock Interactions in a Transonic Turbine Stage,* AGARD, 68th Propulsion and Energetics Panel Meeting, Transonic and Supersonic Phenomena in Turbomachines, Munich (Neubiberg) Germany, 10-12 Sept., 1986.

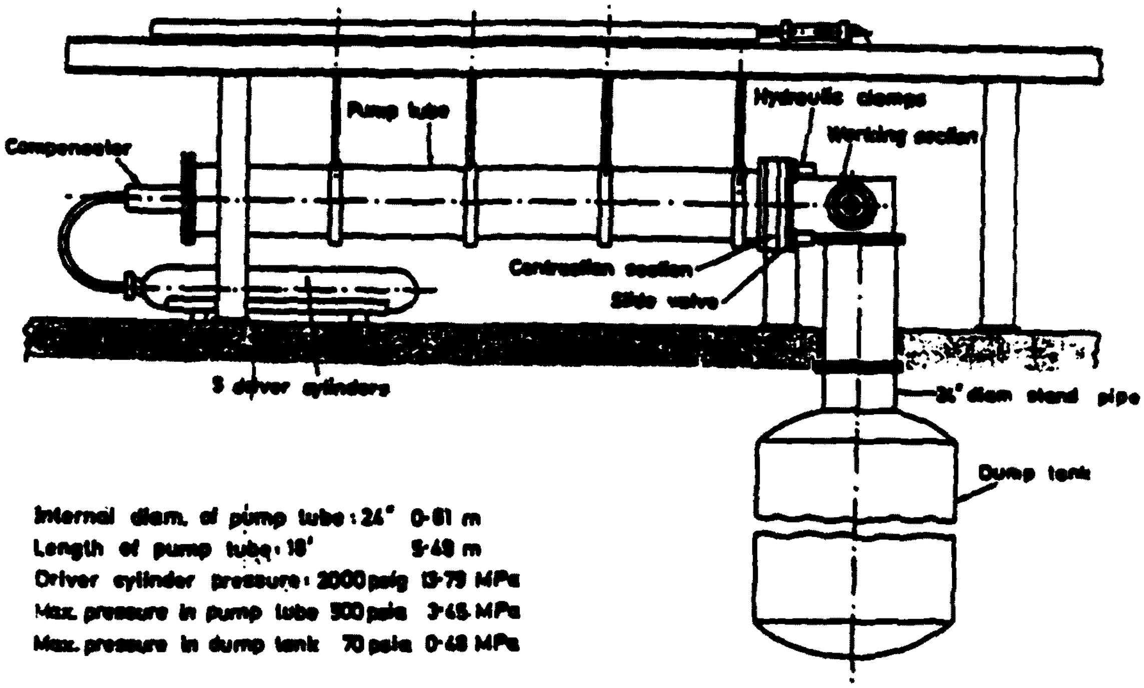

General arrangement of OUEL transient cascade facility.

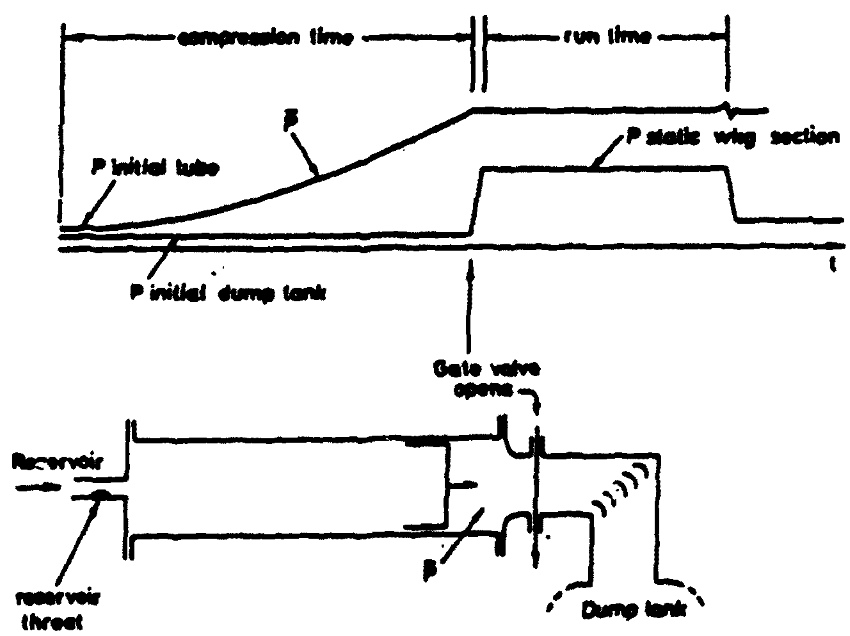

Idealised pressure-time history during compression. Gate valve is opened when pressure in pump tube $\bar{P}$ reaches predetermined value.

Figure 1. Oxford University Light Piston Isentropic Compression Cascade Facility

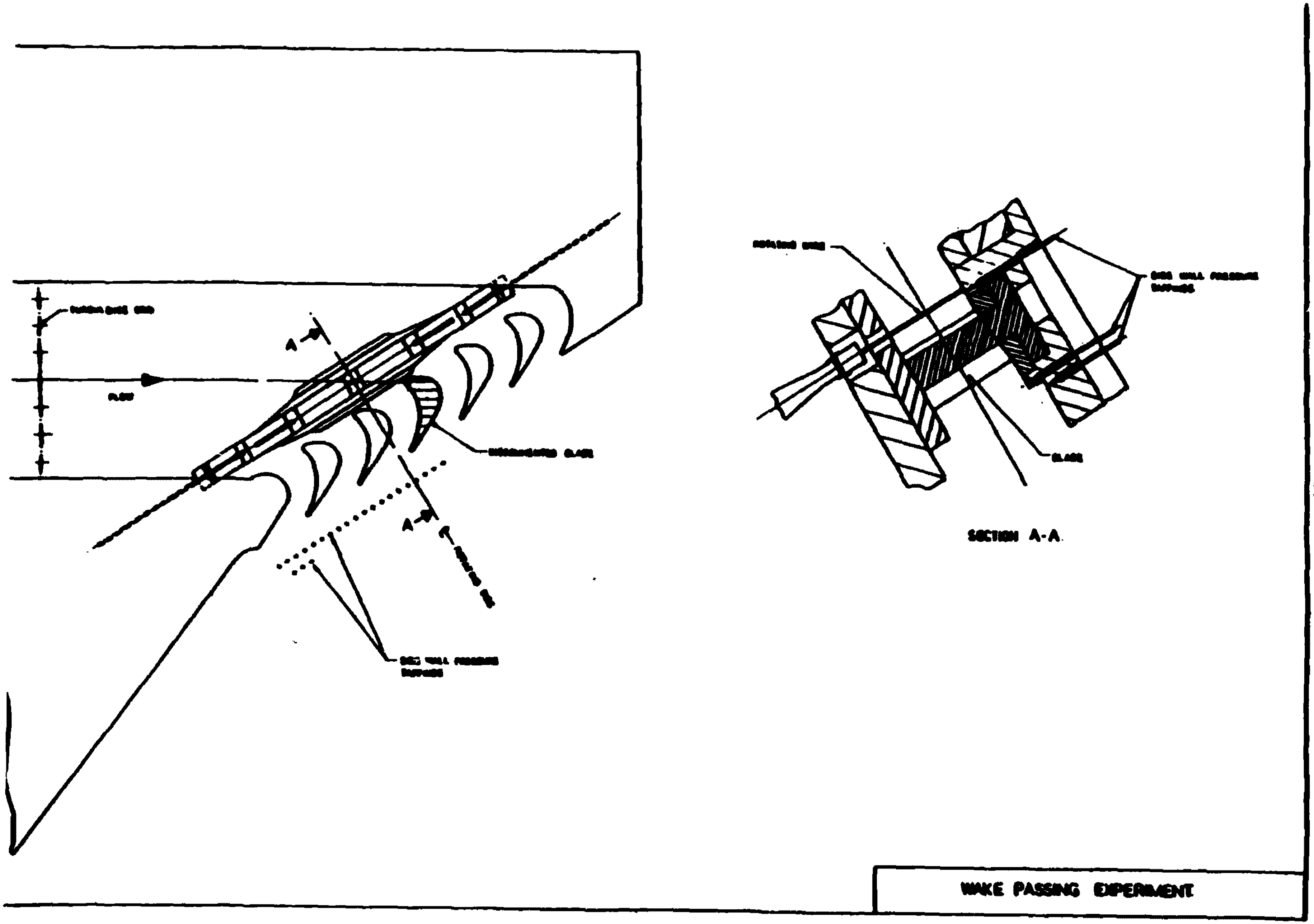

Figure 2. Rotating Bar Wake Generator for Oxford Cascade

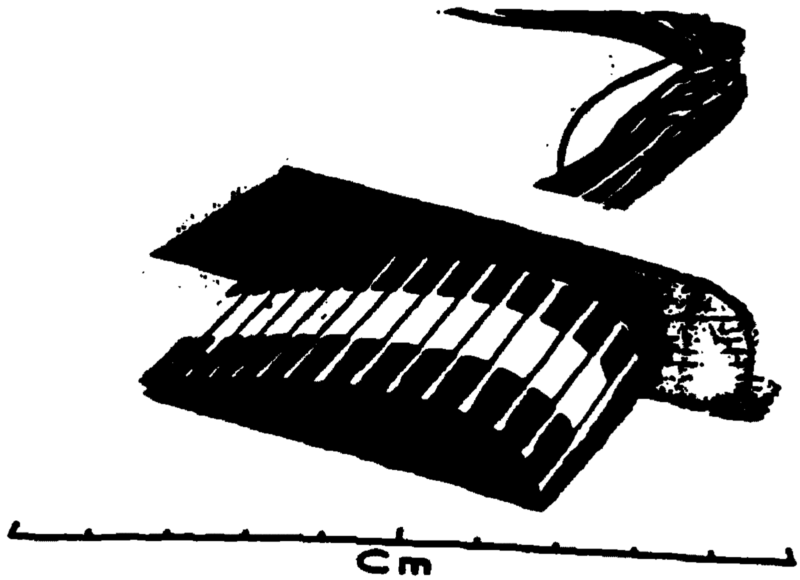

NGV in machineable glass ceramic.

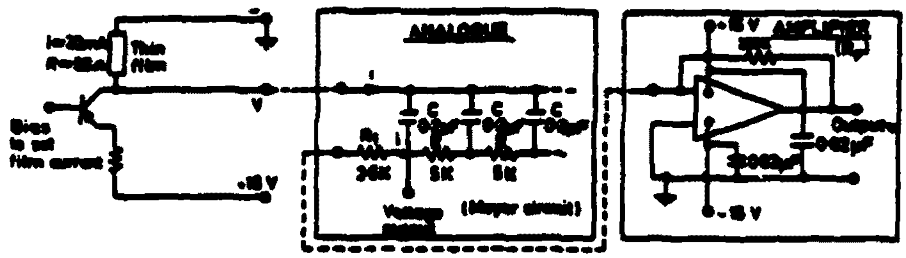

Transistor constant current supply for thin film resistance thermometers, analogue circuit and current-to-voltage converter.

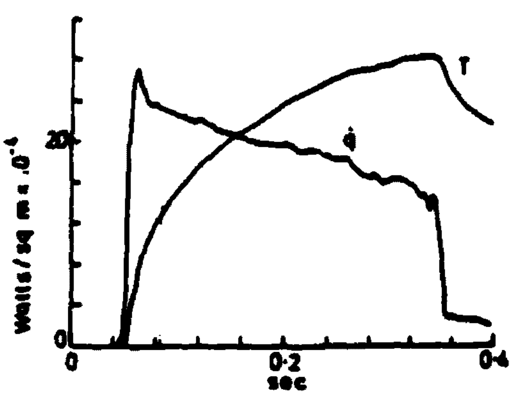

Variation of surface temperature T and heat transfer rate q̇ during run.

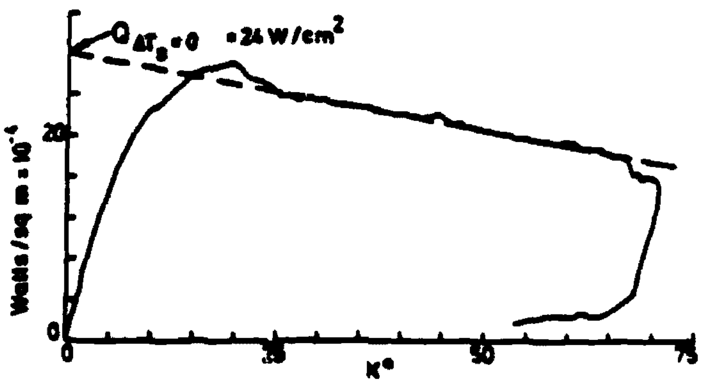

Heat transfer rate versus surface temperature.

Figure 3. Heat Transfer Instrumentation

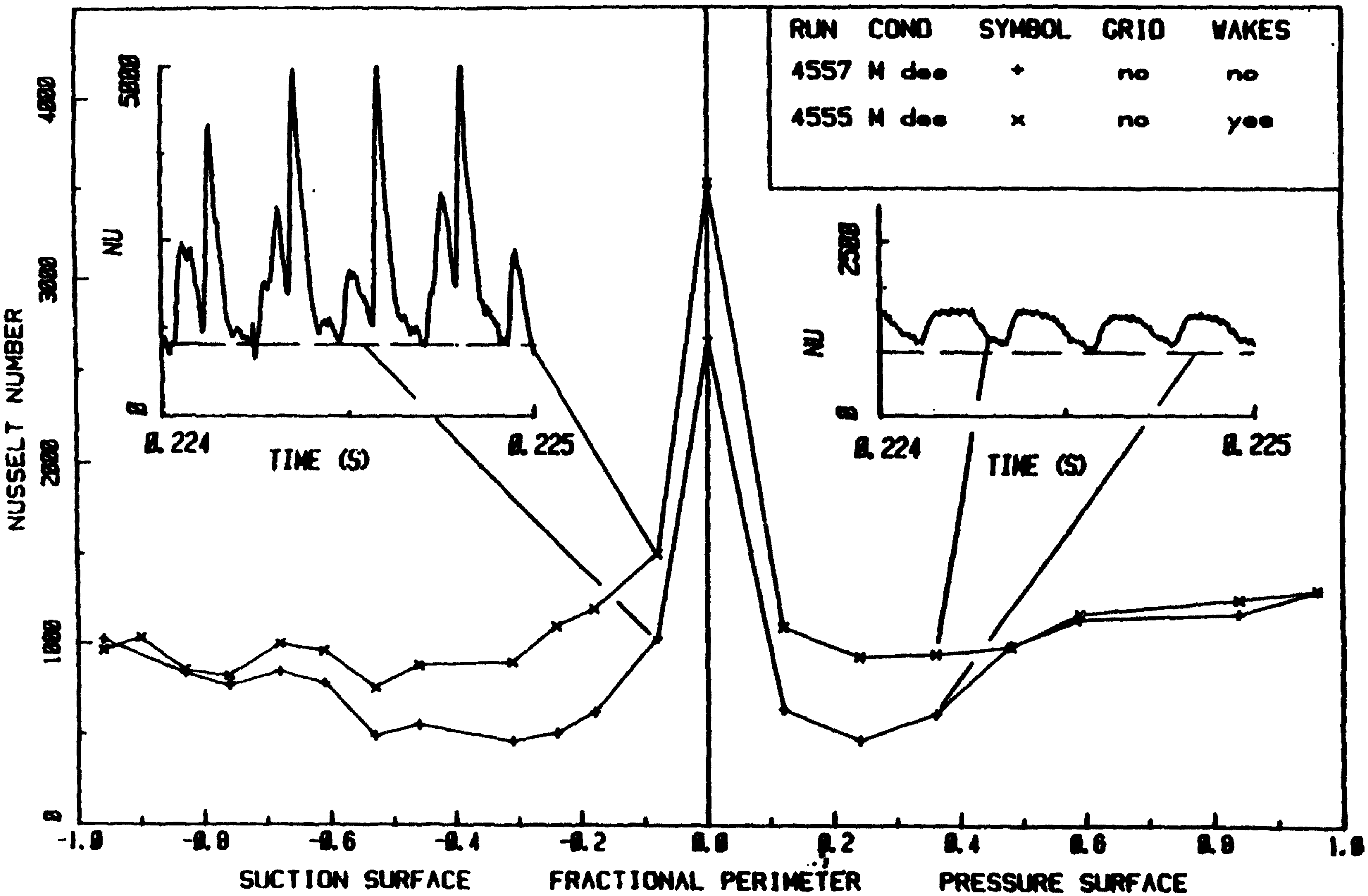

Figure 4. Mean and Instantaneous Heat Transfer With and Without Wake Passing Events (Ref. 6)

Appendix A

Paper to be Presented to ASME/JSME Thermal Engineering
Joint Conference
22-27 March, 1987, Honolulu, Hawaii

Unsteady Interaction Effects on a Transitional Turbine Blade Boundary Layer

D. A. Ashworth
Rolls-Royce plc, Derby, England

J. E. LaGraff
Syracuse University, Syracuse, N.Y., U.S.A.

D. L. Schultz
The University of Oxford, England

ABSTRACT

Results are presented illustrating the detailed behaviour of the suction surface boundary layer of a transonic gas turbine rotor in a 2-D cascade under the influence of both freestream turbulence and simulated nozzle guide vane wakes and shocks. The instrumentation included thin film resistance thermometers along with electrical analogues of the 1-D heat conduction equations to obtain wide bandwidth heat transfer rate measurements in a short duration wind tunnel. This instrumentation provides sufficient time resolution to track individual wake and shock related events and also the turbulent bursts of a transitional boundary layer. Wide bandwidth surface pressure transducers and spark Schlieren photography were used in support of these heat transfer measurements. The results showed there to be a direct relationship between the passage of wake disturbances and transient surface heat transfer enhancements. It was possible to track both wake and transitional events along the surface and to compare these with the expected convection rates. Analysis of the signals allowed direct calculations of intermittency factors which compared well with predictions. Additional effects due to a moving shock/boundary layer interaction were investigated. These resulted in marked variations in heat transfer rate both above and below the laminar values. These excursions were associated with separation and re-attachment phenomena.

NOMENCLATURE

- a = Sound speed
- C_t = Tangential (or true) chord
- k = Thermal conductivity (W/mK)
- $\dot{q}$ = Heat transfer rate (W/m²)
- K = Acceleration parameter, $\frac{\nu}{U^2}\frac{dU}{dx}$
- M = Isentropic Mach number
- Nu = Nusselt number
- R = Radius of curvature (mm) or the gas constant (J/kgK)
- Re = Reynolds number (based on inlet total conditions, isentropic exit Mach number and tangential chord)
- s = Blade surface perimeter
- t = Time
- T = Temperature (K)
- Tu = Turbulence level = u'/U
- u' = Fluctuating velocity (m/s)
- U = Velocity (m/s)
- V = Voltage
- P = Pressure
- x = Surface distance from the leading edge
- β = Gas angle (measured from the axial direction)
- γ = Ratio of specific heats
- $\bar{\gamma}$ = Intermittency factor
- μ = Viscosity (kg/ms)
- ν = Kinematic viscosity = μ/ρ
- ρ = Density (kg/m³)

Subscripts

- ∞ = Freestream
- o = Total
- 1 = Inlet
- 2 = Outlet
- m = Parameter at the selected measuring instant
- rel = Condition relative to the rotating bar

INTRODUCTION

The need to understand the processes by which transition takes place in a boundary layer and its susceptibility to disturbance by events occurring in the freestream have led to a growing amount of research much of it aimed towards the gas turbine industry. An increase in the level of freestream turbulence has been shown to encourage the transition process (Blair, 1982 Rued and Wittig, 1984) following the turbulent spot models proposed by Schubauer and Klebanoff (1956). The effects of intermittent changes in flow conditions such as those caused by the Nozzle Guide Vane (NGV) and rotor blade interactions have also been shown to have significant influences on heat transfer rate to the blades, as detailed by Dunn (1985) and Doorly (1983). The tests reported in this paper investigate both the transitional phenomena and the influence of a simulated NGV on a rotor blade suction surface boundary layer. The use of wide bandwidth heat transfer instrumentation

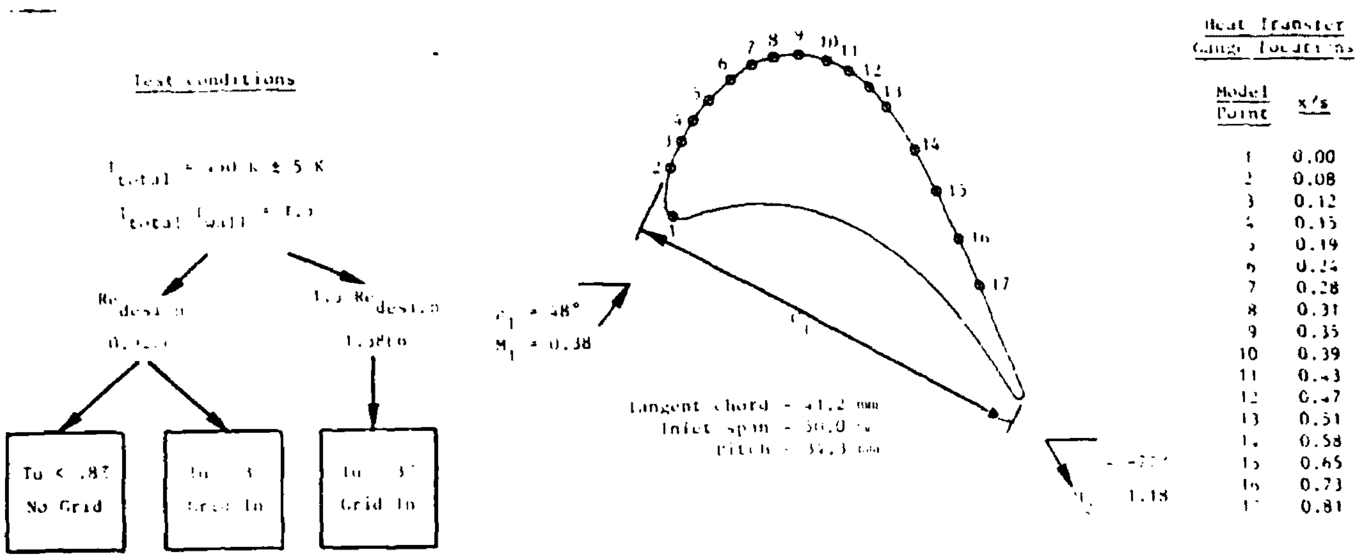

Figure 1 - Instrumented Model Details and Test Conditions.

enables individual events such as turbulent spots developing in the transitional boundary layer to be easily identified, at freestream conditions corresponding to the gas turbine environment in terms of Mach number, Reynolds number and gas-to-wall temperature ratio.

Experimental Approach

The present study was carried out on a transonic gas turbine rotor blade in the Isentropic Light Piston Tunnel (ILPT), as described by Schultz et al.(1977). The ILPT is a short duration facility which for a typical run time of about 0.5 seconds gives a gas-to-wall temperature ratio of 1.5 . For these tests a 5-bladed cascade of 50 mm inlet span was used with a Mach number of 0.38 at inlet and 1.18 at the exit plane with a corresponding Reynolds number of 0.92 x 10^6. The freestream turbulence level could be varied from a background level of less than 0.8% to a "high" level of about 3% by use of a grid of 2 mm bars placed 208 mm upstream of the cascade inlet plane. The operating conditions are detailed in Figure 1, using the definitions :

$$Re = \text{Reynolds number} \qquad = \frac{\rho U_2 C_t}{\mu}$$

with viscosity derived from Sutherland's law.

$$M = \text{Isentropic Mach number} = U/a_s$$

$$\text{where sound speed } a_s = \sqrt{\gamma R T_s}$$

The position of the heat transfer instrumentation is also shown in Figure 1, with the 17 thin film gauges spaced around the suction surface. For these tests the gauges were spaced 2.5 mm apart from 8% to 50% of the surface perimeter of 64.2 mm, with a 5 mm spacing thereafter. The gauges were 0.5 mm wide and covered 4 mm of the span, compared with the 10 mm gauges used previously in the cascade to enable smaller three-dimensional events to be observed. The gauge effectively averages the heat transfer rate along its length, thus reducing the magnitude of any events of size smaller than the film coverage. Heat transfer rate was obtained using a well-established technique (Schultz and Jones, 1973) by using electrical analogues of the semi-infinite conduction equation to give a direct measurement of heat transfer rate with a bandwidth of 100 kHz, as described by Oldfield et al.(1984). Wide bandwidth surface-mounted pressure transducers (Kulite type XCQ-062-50D) were used, together with spark Schlieren photographs in the analysis of the data.

In order to further characterise the freestream conditions, constant temperature hot wire anemometer measurements were made at the channel centre line at the entrance plane of the cascade leading edge. The probe used was a DISA P11 5 micron platinum coated tungsten wire of 2 mm length and connected to a DISA 55D01 constant temperature anemometer bridge tuned to a bandwidth of greater than 50 kHz.

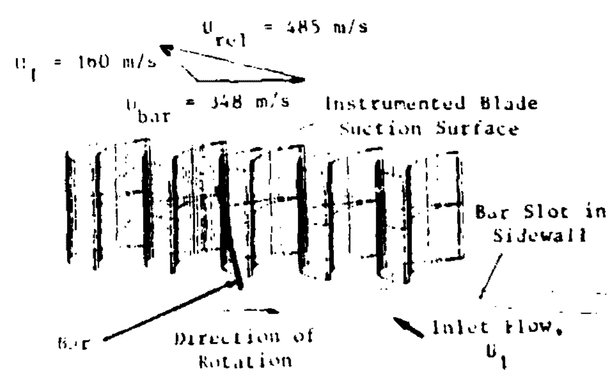

Figure 2 - The Cascade with Rotating Bar Configuration.

The heat transfer results are presented in Nusselt number form, i.e.

$$Nu = \frac{\dot{q}_m}{(T_o - T_m)} \frac{C_t}{k}$$

with gas conductivity k = 0.0047 + 7x10^{-5} T_o in W/mK

The effects of the NGV-rotor interaction were simulated by 2 mm diameter bars attached to a disk spun upstream of the cascade, as described by Doorly and Oldfield (1985b), and illustrated in Figure 2. By this means it is possible to simulate the inlet perturbation in the rotor relative frame for the cascade, to give the correct NGV wake orientation and scale. This method was used by Ashworth et al.(1985) for the same profile at an inlet angle of 58° with a bar-to-cascade mid-span pitch ratio of 1.7 representative of a realistic turbine design. The present study reduced the number of bars to 2 giving a pitch ratio of 13.4 so that individual periodic disturbances could be identified, giving a bar-passing frequency of 740 Hz. In the fast sampling period of 6 milli-seconds it was possible to capture 4.4 bar-passing cycles, so that the repeatability of events could be determined.

The data was acquired in several ways:

(i) Slow samples were taken at 500 Hz using a 64-channel DataTranslation DT1711 A-D board, with a PDP11/34 controlling this acquisition and the tunnel housekeeping channels establishing the steady flow conditions. From this data mean values of heat transfer rate are deduced by choosing a time interval around a measure point in the run for which conditions are steady (Oldfield et al., 1978).

(ii) A Datalab DL2800 transient recorder was used to acquire 16 channels of 4096 points at a sampling rate of 500 kHz at a time in the run around the measure point. These results form the basis of the transient analysis in this paper.

(iii) Schlieren photographs stored a "snapshot" of the flowfield as an aid in interpretation of the surface measurements.

STEADY BASELINE FLOW CONDITIONS

Measurements of the mean aerodynamic and heat transfer properties of the rotor cascade are given in Figure 3 for the suction surface at the test condition of the present experiment. The heat transfer coefficient given as Nusselt number is seen to increase at and near the leading edge as expected with higher freestream turbulence and blade Reynolds numbers (Lowery and Vachon, 1975). As the boundary layer develops along the surface the heat transfer rate in the high and low freestream turbulence cases merge together at essentially the laminar level. The low turbulence case heat transfer rate (Tu < 0.8%) remains laminar to the x/s position of 0.8 whereas in the high turbulence case (Tu = 3%) begins to increase in proportion (as will be shown in the following section) to increasing levels of turbulent spot intermittency. In the high Reynolds number (and high freestream turbulence) case the heat transfer rate never comes down to the laminar level and begins climbing due to transitional intermittency soon after the x/s = 0.15 location. The freestream velocity as determined by surface pressure measurements increases gradually along the entire blade surface matching very well the values from a blade-to-blade prediction program. It should be noted that the local flow velocity becomes supersonic by an x/s = 0.34. The predicted acceleration parameter drops to a very low (favourable) value very early on the blade surface and becomes only slightly adverse beyond the x/s position of 0.63. This is near the rearmost point where wide bandwidth transient heat transfer data are collected and reported on in the following section. It is also near the point where the trailing edge shock wave from the adjoining

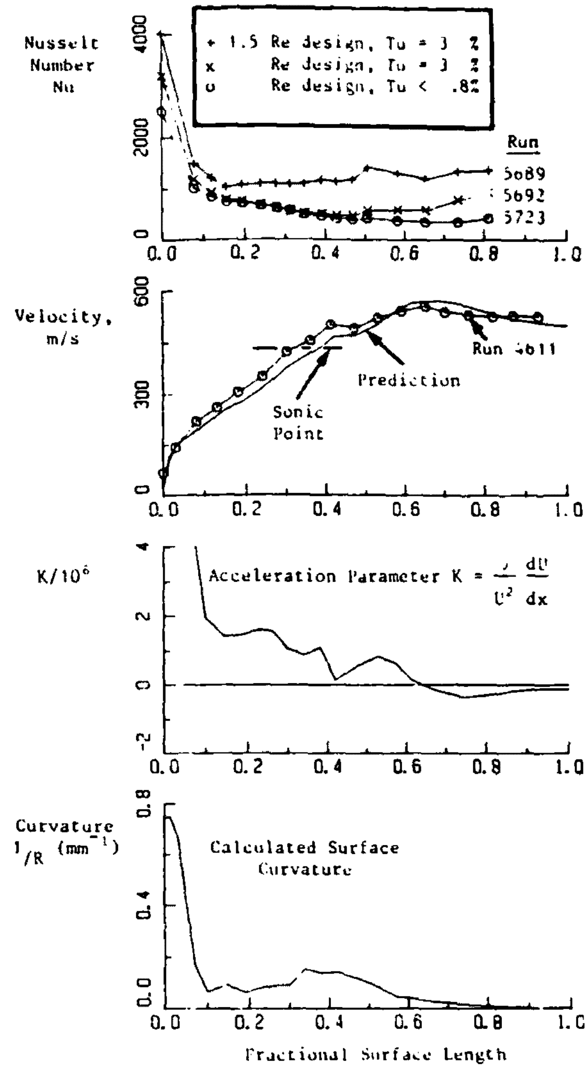

Figure 3 - Baseline Surface Conditions.

rotor blade is expected to encounter the suction surface. Transitional high speed data is not reported past this point, although no significant change in the mean heat transfer coefficient was observed. The calculated surface curvature is also shown to reach a low value a short distance from the leading edge and to remain there to the trailing edge.

NATURAL TRANSITION ON A TURBINE BLADE SURFACE BOUNDARY LAYER

Wide bandwidth heat transfer signals from surface thin films clearly illustrate the important difference between the low and high freestream turbulence cases as shown in the transient recorder traces of Figure 4. The heat transfer rate in the low turbulence case (Run 5723) remains quiet (laminar) throughout the entire measuring range of the transient data (to x/s = 0.65). The high freestream turbulence case, while starting somewhat higher than the laminar case, becomes increasingly

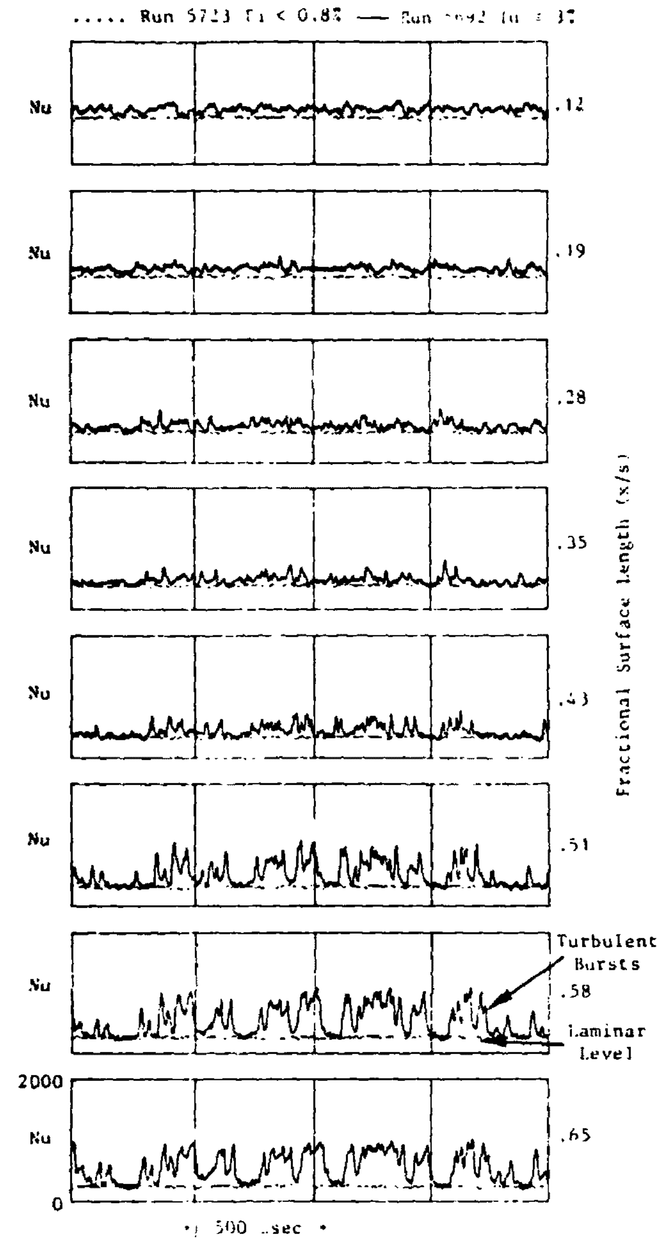

Figure 4 - **Measured Nusselt Number. The Effect of Free-stream Turbulence on Natural Transition. (The Vertical Scale for Each Trace Range from 0 to 2000 in** *Nusselt Number.***)**

dominated by *sharp* transient events (consistent with turbulent spot development, amplification and gradual merger) which raise the heat transfer coefficient instantaneously to high turbulent levels until finally the Nusselt *number* signals become more characterised by the steady turbulent levels. It is clearly seen at the $x/s = 0.65$ point that the *flow* is at the turbulent level more than half of the time dropping precisely to the undisturbed laminar values between the turbulent events. This process starts earlier and proceeds faster for the higher Reynolds number case (not shown here).

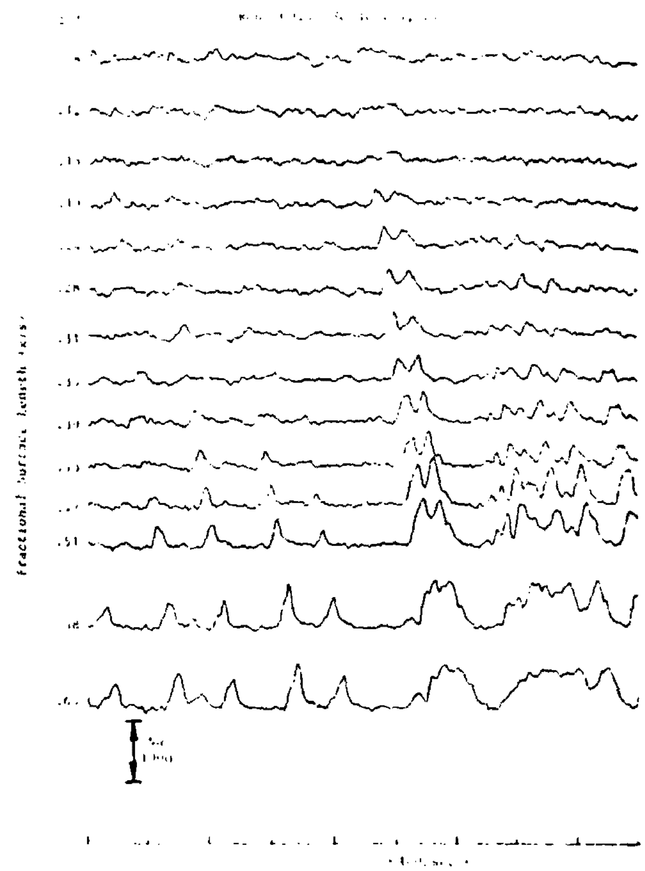

Figure 5 - Natural Transition Heat Transfer Progression *Along* **the Model Surface.**

The physical process of turbulent spot development growth and merger is dramatically illustrated in Figure 5 in which a time synchronised overlay of each instantaneous heat transfer record is shown. In this figure the growth and rearward convection of individual turbulent spots is clearly seen as they move along the surface, again with the levels between spots dropping to the laminar values. This growth pattern suggested a procedure for the quantitative analysis of the degree of turbulent activity and the convection rates of individual spots. Figure 6 shows expanded time records of four consecutive positions. By selecting a turbulent threshold level slightly above the laminar value the amount of time that the digital signal is above this value compared to the total time of the trace can be used to define an intermittency value of the boundary layer at any x/s position as

$$\bar{\gamma} = \frac{\sum_{i=1}^{n} \Delta t_i}{t_2 - t_1}$$

between any time interval $t_2 - t_1$. Also clearly seen in Figure 6 is the regular time delay for the turbulent spot to move *from* one position to the next. If one were to shift the signals closer together, adjacent heat transfer records would be seen to be nearly co-incident

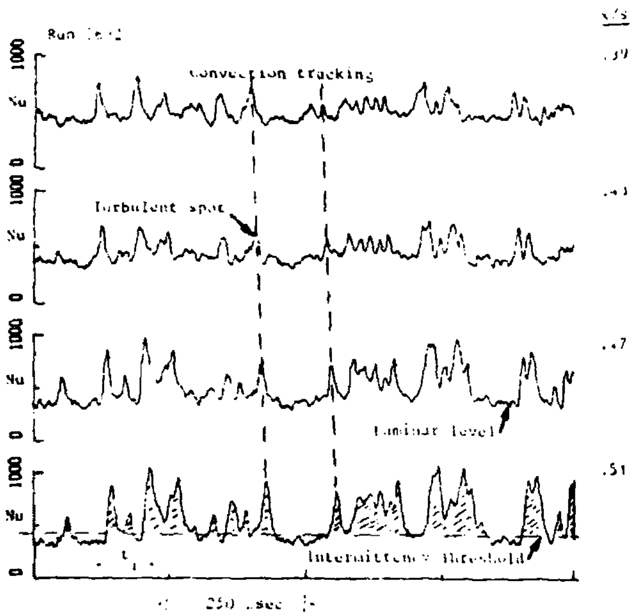

Figure 6 - Turbulent Spot *Convection* Rate *and* Intermittency Calculation.

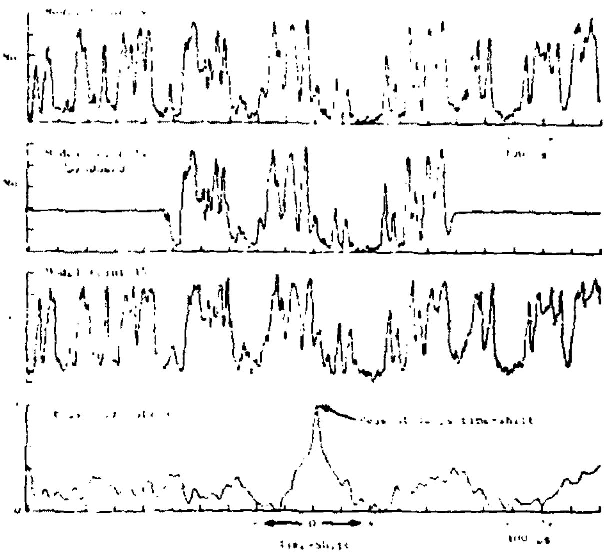

Figure 8 - Example of Cross-Correlation Analysis o Adjacent Heat Transfer Signals in a Tran sitional Boundary Layer (using a progr developed by Doorly (1983)).

except for a very slight but regular displacement in the direction of increasing time. Figure 7 presents the value of the intermittency calculated in this way for the two conditions of design and 1.5 x design Reynolds number each with the turbulence grid in place. The rise of the intermittency above zero and the following rapid rise is seen to follow for some time the predicted values, reaching a value near unity for the high Reynolds number case. The *prediction code is one* developed from the method described in Patankar and Spalding (1970) incorporating a model for mixing in *freestream* turbulence into the boundary layer, and allowances for curvature and changes in freestream conditions during transition, outlined by Forest(1977).

The convection rate for turbulent spots was estimated by measuring time delays for individual well-*defined* spots an from cross-correlation analysis of adjoining thin film signals. Using a cross-correlation analysis

as *shown* in Figure 8, two signals (each containing 102 data points) are compared for various values of tim delay and the peak value determined. *Correlatic* coefficients of over 0.9 were found for the highl transitional traces late on the blade surface. The tim delay was then used with the known film spacing t estimate a mean convection velocity of the discret events associated with transition. These values ar plotted in Figure 9 assuming a spot origin near th location where the intermittency rises above zero. F comparison, the spot trajectories are compared wi curves moving at various fractions of the bla freestream velocities. The mean convection rates a seen to be between 0.7 and 0.8 of the local freestre velocity, as observed in low speed transitional bounda layers.

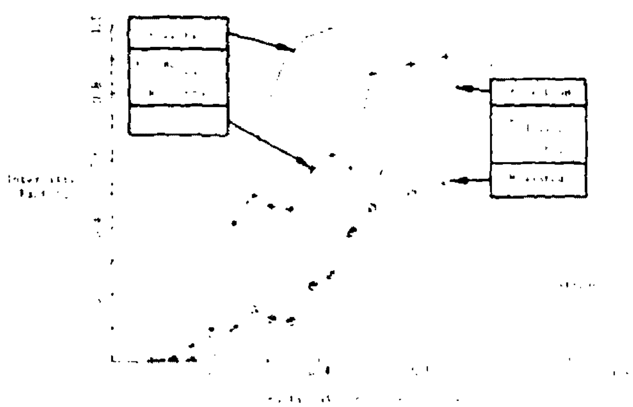

Figure 7 - *Intermittency Measurements and Predictions* for Natural Transition.

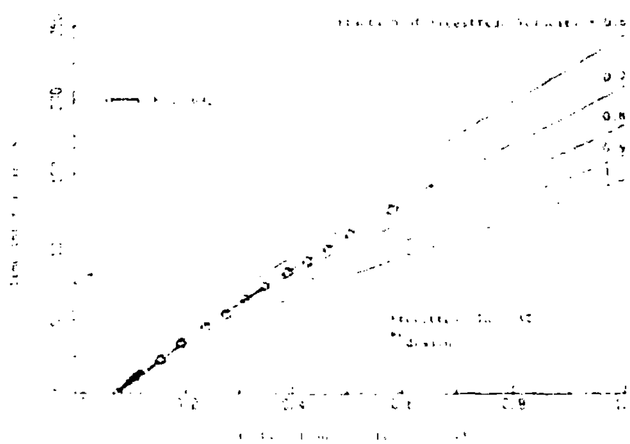

Figure 9 - Measured Convection Rate of Turbulent Spot by Cross-Correlation Analysis Compared wit Fractions of the Local Freestream Velocity.

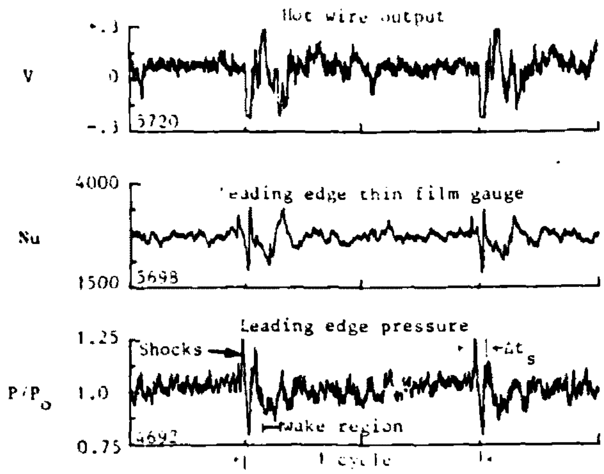

Figure 10 - Comparison of the Effect of Unsteady Wakes and Shocks on a Freestream Hot-wire Output with Leading-Edge Pressure and Heat Transfer Rate Measurements.

NGV WAKE AND SHOCK WAVE EFFECTS

The reaction of an otherwise laminar boundary layer to a higher level of isotropic freestream turbulence has been detailed above. Clearly transition was induced by these velocity fluctuations of about 3%. In this section results are presented of tests at the design Reynolds number (0.92 x 10⁶) with NGV wake and shock structures simulated by the bar-passing apparatus described in the Introduction.

The intermittent perturbations to the inlet flow caused by the simulation are shown in the high freestream turbulence case in Figure 10 in terms of hot-wire output from a probe mounted in the freestream inlet plane at mid-passage, and blade surface leading-edge measurements of pressure and heat transfer rate. This data is normalised with respect to 2 cycles of the bar-passing event, so that it is possible to relate information from different runs in terms of cycle fraction. The signals show a background turbulent level extending over about 60% of the cycle characterised by a similar type of signal to that obtained with no rotating bars. All three signals have a periodic component at bar-passing frequency with two characteristic parts:

(i) Over about 6% of the cycle rapid changes in level of the order of 5 to 10 μs rise and fall times are observed. The pressure signal varies by +/- 25% and the heat transfer rate by approximately +/- 50%. This disturbance is attributed to shock waves generated as the bar sweeps past the cascade. By examination of Schlieren photographs of this flow, an example of which is given as Figure 11, the nature of the NGV simulated shock structure can be determined. Clearly two shocks are associated with one bar-passing event, the bow and recompression shocks that would be expected at the bar relative Mach number in steady flow. The separation time between these shocks is approximately 75μs, marked as Δt_s in Figure 10, and is seen to correspond to the time interval between the sharp falls in level to the adjacent sharp peak.

(ii) Following these rapidly changing events, a second less marked change in level associated with the wake is also visible over about 10% of the cycle, denoted as the "wake" region in Figure 10.

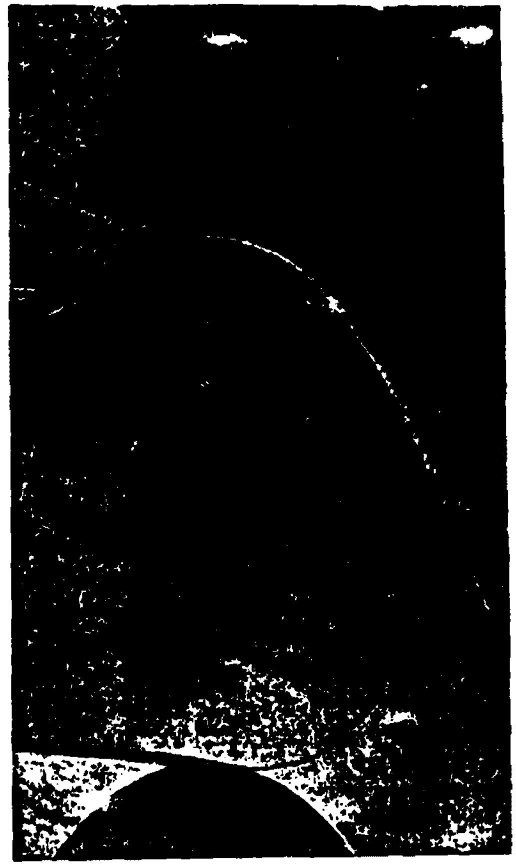

Figure 11 - Schlieren Photograph Showing the Intersection of the Moving Bar Shock Waves with the Turbine Blade Suction Surfaces.

It is possible to analyse the reaction of the blade boundary layer to the wake and shock perturbations by investigation of the sequence of time-resolved Nusselt number plots given in Figure 12. There is a constant spacing of 5 mm between the thin film gauges, starting with gauge 3 at an x/s value of 0.12 through to gauge 15 at x/s=0.65 . The high freestream turbulence case with wakes and shocks present (Figure 12(a)) is markedly different to the naturally transitional boundary layer over the first 35% of the surface, with similar rapid rises and falls in Nusselt number to the perturbations evident in Figure 10. This shock related event occurs on the early suction surface due to a shock/boundary layer interaction starting at gauge 9, close to the crown of the suction surface. Examination of Schlieren photographs (such as Figure 11) indicates that the shocks first interact with the boundary layer near to gauge 9, the reflection point moving towards the leading-edge as the bar moves in the same direction. This is visible on the early gauges on Figure 12(a), occurring first on gauge 9 then moving gradually through gauges 7 and 5 and finally showing on gauge 3. The rapid drop in surface Nusselt number is attributed to an unsteady separation and the rise to a turbulent reattachment both caused by the shock boundary layer interaction. The effect of the wake is not clearly discernable in Figure 12(a) and to aid in identification of this the bars were rotated at a lower speed such that the bar relative Mach number was subsonic. The results

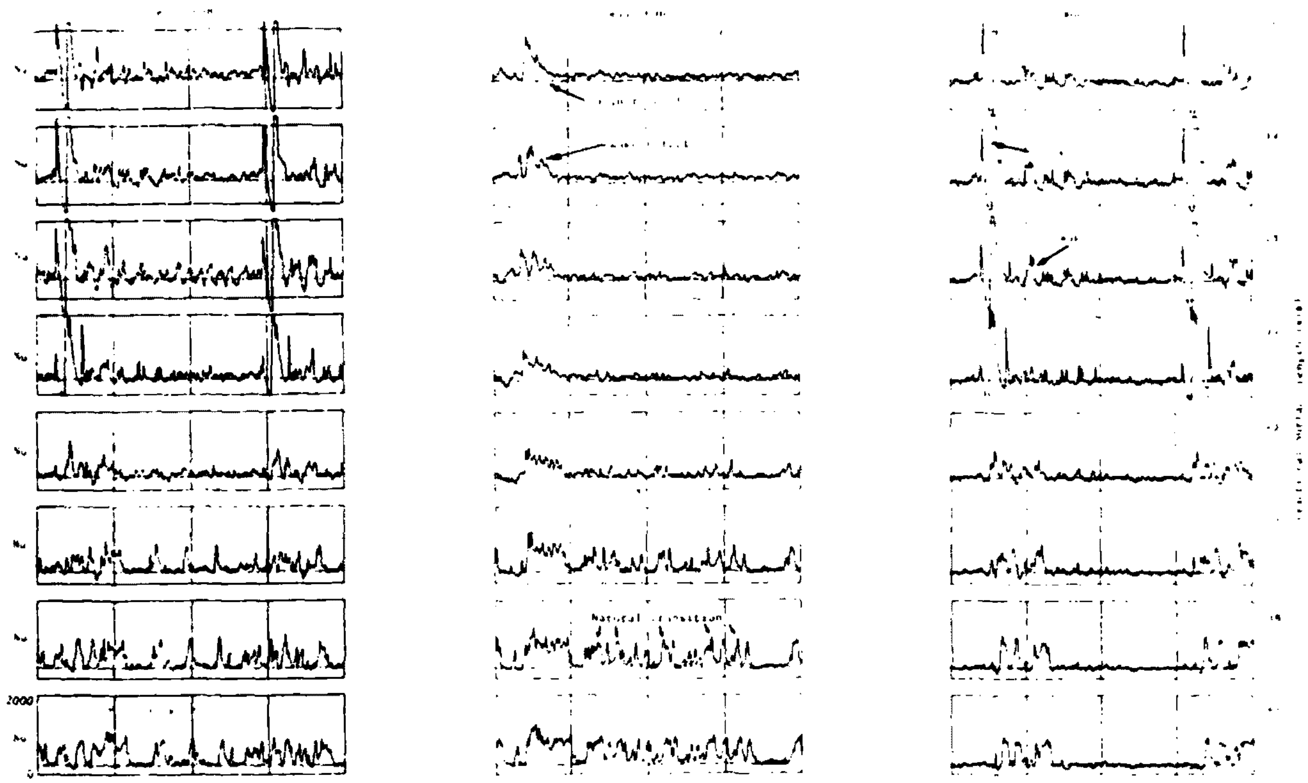

(a) (b) (c)

Figure 12 - Comparison of the Effects of Shock and Wake-Passing Eve... with Undisturbed Laminar Boundary Layer Heat Transfer.

of this are shown as Figure 12(b) with a much more clearly identifiable enhancement in heat transfer due to this wake. This extends to the later gauges of the surface causing the boundary layer to be fully turbulent over the extent of the wake. In Figure 12(c) the background turbulence was reduced to less than 0.8% and the periodic disturbances due to the bar-passing events are more clearly evident. The early suction surface has shock-related phenomena extending well into the cycle period but apparent oscillations in Nusselt number moving with the shock. Also apparent from Figure 12(c) is the intermittent nature of the turbulence induced in the boundary layer by the wake and shock interaction, as the boundary layer clearly returns to its undisturbed laminar value between the periodic events. The heat transfer enhancement due to the wake is clearly evident along the whole surface.

As an aid to quantifying the periodic effects due to wake and shock passing phenomena the RMS fluctuations caused by the disturbances in the boundary layer are plotted for each gauge in Figure 13. The baseline run (marked as x-x-x) shows a constant low RMS level as would be expected, and the higher freestream turbulent case shows a steady increase following the boundary layer intermittency factor. With just wakes present as was shown in Figure 12(b) a general enhancement of this RMS value is evident over the whole surface, whereas with the shocks present the fluctuation is much enhanced on the earlier surface but returns to undisturbed values towards the later gauges. The values come close together at an x/s of 0.43 for all the bar-passing cases, indicating the extent of the shock interaction region.

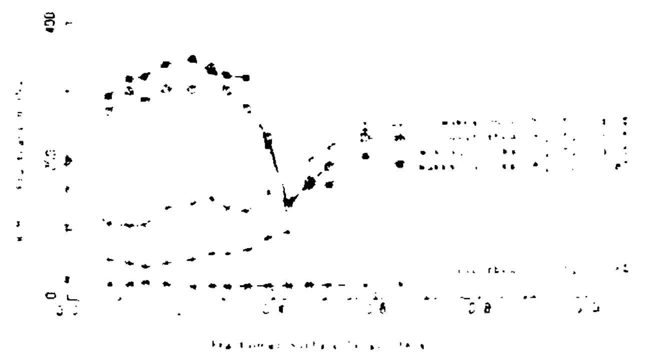

Figure 13 - Comparison of RMS Nusselt Number Fluctuations over the Blade Surface for Various Disturbances at the Design Reynolds Number.

CONCLUSIONS

It has been established during the course of this study that the Isentropic Light Piston Tunnel facility combined with the wide bandwidth/high sampling rate heat transfer instrumentation has proved capable of tracking very rapidly progressing unsteady events in a transonic boundary layer. Operating under a simulated unsteady gas turbine rotor environment, sensitive detection and precision tracking of transient shock, wake and boundary

layer transitional events was accomplished. Detailed observation of the heat transfer signals confirmed a classical model of the transition process, viz. the sudden appearance of sharp spikes of turbulence which multiply, grow and track downstream at a rate less than the freestream velocity until gradually merging to form a completely turbulent boundary layer. The tracking of turbulent spots at these high temperature transonic flow conditions has not been reported before to the best of the authors' knowledge.

A second major finding of this study was the observation that the strong unsteady interaction of a double shock and a simulated NGV wake with the rotor boundary layer did not have any measurable "long term" effects apart from the strong excursion in heat transfer associated with the actual passing of the shocks and wake. The heat transfer fluctuation levels were essentially unchanged far removed from the disturbance (in time) and nearly identical at the rearmost measuring point except for a turbulent patch associated with the shock/wake event itself.

The interaction of the shocks and wake with the rotor establishes in more detail the earlier observation of Ashworth et al.(1985) and Doorly and Oldfield (1985a) of strong changes in local heat transfer coefficient. The tracking of the interaction over the surface could be followed with some precision with the time resolution of the instrumentation used. Further analysis of shock and wake interactions is reported by the authors in Schultz et al.(1986) along with some prediction models of the interaction dynamics.

ACKNOWLEDGEMENTS

The authors wish to acknowledge the invaluable contributions to this paper made by M. L. G. Oldfield during many discussions throughout the course of the work. We would also like to thank M. J. Rigby and A. B. Johnson for their help in collecting some of the data. Professor LaGraff would also like to acknowledge the financial support of the U.S. Air Force Office of Scientific Research under grant number 85-0295 and the Division of International Programs of the National Science Foundation for providing a travel grant (INT-8509407) to facilitate the collaborative research programme.

REFERENCES

Ashworth, D. A., LaGraff, J. E., Schultz, D. L. and Grindrod, K. J., 1985, "Unsteady Aerodynamics and Heat Transfer Processes in a Transonic Turbine Stage," J. Eng. for Gas Turbines and Power, Vol. 107, pp. 1022-1030.

Blair, M. F., 1982, "Influence of Freestream Turbulence on Boundary Layer in Favourable Pressure Gradients," J. Eng. for Power, Vol. 104, No. 4, pp. 743-750.

Doorly, D. J., 1983, A Study of the Effect of Wake Passing on Turbine Blades, D.Phil. Thesis, University of Oxford.

Doorly, D. J. and Oldfield, M. L. G., 1985a, "Simulation of the Effects of Shock Wave Passing on a Turbine Rotor Blade," J. Eng. for Gas Turbines and Power, Vol. 107, No. 4, pp. 998-1006.

Doorly, D. J. and Oldfield, M. L. G., 1985b, "Simulation of Wake Passing in a Stationary Turbine Rotor Cascade," J. Propulsion and Power, Vol. 1, No. 4, pp. 316-318.

Dunn, M. G., 1985, "Turbine Heat Flux Measurements: Influence of Slot Injection on Vane Trailing Edge Heat Transfer and Influence of Rotor on Vane Heat Transfer," J. Eng. for Gas Turbines and Power, Vol. 107, No. 1, pp. 76-83.

Forest, A., 1977, "Engineering Predictions of Transitional Boundary Layers," AGARD Conference Proceedings, Laminar-Turbulent Transition, CP-224, Paper No. 22.

Lowery, G. W. and Vachon, R. I., 1975, "The Effect of Turbulence on Heat Transfer from Heated Cylinders," Int. J. Heat Mass Transfer, Vol. 18, pp. 1229-1242.

Oldfield, M. L. G., Jones, T. V. and Schultz, D. L., 1978, "On-Line Computer for Transient Turbine Cascade Analysis," IEEE Transactions on Aerospace and Electronic Systems, Vol. AES-14, No. 5, pp. 738-748.

Oldfield, M. L. G., Burd, H. J. and Doe, H. G., 1984, "Design of Wide Bandwidth Analogue Circuits for Heat Transfer Instrumentation in Transient Tunnels," Papers from the 16th ICHMT Symposium on Heat and Mass Transfer, Dubrovnik, pp. 233-258.

Patankar, S. V. and Spalding, D. B., 1970, Heat and Mass Transfer in Boundary Layers, 2nd Edit., Intertext Book, London.

Rued, K. and Wittig, S., 1984, "Freestream Turbulence and Pressure Gradient Effects on Heat Transfer and Boundary Layer Development on Highly Cooled Surfaces," J. Eng. for Gas Turbines and Power, Vol.107, pp. 54-59.

Schubauer, G. B. and Klebanoff, P. S., 1956, "Contributions on the Mechanics of Boundary Layer Transition," NACA Report 1289.

Schultz, D. L. and Jones, T. V., 1973, "Heat Transfer Measurements in Short Duration Hypersonic Facilities," AGARDOGRAPH No. 165.

Schultz, D. L., Jones, T. V., Oldfield, M. L. G. and Daniels, L. C., 1977, "A New Transient Cascade Facility for the Measurement of Heat Transfer Rates," AGARD Conference Proceedings, High Temperature Problems in Gas Turbine Engines, CP-229, Paper No. 31.

Schultz, D. L., Ashworth, D. A., LaGraff, J. E., Johnson, A. B. and Rigby, M. J., 1986, "Wake and Shock Interactions in a Transonic Turbine Stage," AGARD 68th(B) Specialists' Meeting Transonic and Supersonic Phenomena in Turbomachines, Paper No. 3, Neubiberg, Germany.

Appendix B

Paper Presented at AGARD 68th Propulsion and Energetics
Panel Meeting - Transonic and Supersonic Phenomena in Turbomachines
10-12 September, 1986, Neubiberg, W. Germany

WAKE AND SHOCK INTERACTIONS IN A TRANSONIC TURBINE STAGE

D. L. Schultz[*], D. A. Ashworth[+], J. E. LaGraff[o], M. J. Rigby[+], A. B. Johnson[*]

Abstract

The strong trailing-edge shock waves from the nozzle guide vanes of transonic turbine stages can give rise to interactions with the downstream rotor which are significantly more severe than is the case with lower pressure ratio stages. It is therefore important to study such effects in detail both from the point of view of stage power output and more importantly from that of heat transfer rates. A study has been made of a transonic rotor profile in a static cascade in which the effect of shock wave interaction is simulated by means of an array of bars rotating at the correct speed and spacing upstream of the stationary rotor blades. Detailed heat transfer rate measurements made with rapid response gauges enable the wake and shock phenomena to be separated.

Nomenclature

C_2 = NGV exit velocity, relative bar velocity
C_t = Tangential (or true) chord
k = Thermal conductivity (W/mK)
$\dot{q}$ = Heat transfer rate (W/m²)
M = Isentropic Mach Number (based on local static pressure and inlet total pressure)
Nu = Nusselt Number
Re = Reynolds Number (based on inlet total conditions, isentropic exit Mach Number and tangential chord)
s = Blade surface perimeter
t = Time
T = Temperature (K)
Tu = Turbulence level = $u'/\bar{U}$
u' = Fluctuating velocity (m/s)
U = Velocity (m/s)
V = Rotor relative velocity, cascade inlet velocity
x = Surface distance from the leading edge stagnation point
y_b = Distance in the pitch-wise direction from the spanwise datum position
β = Gas angle (measured from the axial direction)

Subscripts

∞ = Freestream
o = Total
1,2 = Inlet, Outlet
meas = Measuring point
h,m,t = Hub, mean, tip (or tangential in chord definition)
rel = Relative bar condition

---

[*]Department of Engineering Science, University of Oxford, U.K.
[+]Rolls-Royce plc, Derby, U.K.
[o]Department of Mechanical and Aerospace Engineering, Syracuse, U.S.A.

edge. The cascade has a span of 50 mm at blade inlet and 56.095 mm at exit with the expansion on one side only as illustrated in Fig. 1(a). A turbulence grid 208 mm upstream of the cascade provides a level of $u'/\bar{U}$ of approximately 3%. Upstream and downstream static and total pressures were measured routinely to establish the correct cascade operating conditions and are reported in more detail by Ashworth et al.[18]. The operating conditions at the nominal engine design point are given below.

The heat transfer gauges used in this study are conventional thin film surface resistance thermometers widely used for the determination of heat transfer rate in short duration facilities[19]. Data from 22 such gauges were stored in a digital transient recorder sampling up to 16 channels at 500 kHz for each channel or were input directly to the A/D converter at a slower rate of 400 Hz for some of the 64 available A/D channels when time average data only were required, also used for measurements such as inlet and exit static pressures. The locations of these heat transfer gauges on the blade are shown in Fig. 2(a) and given in terms of the surface length 'x' to perimeter 's' from the stagnation point. A more detailed study of the reaction of the suction surface boundary layer to both freestream turbulence and the wake-passing phenomena is also reported below. For this study another blade was instrumented with thin film gauges which were only 4 mm long as compared to 10 mm for the previous tests, and were more closely spaced around the profile, as shown in Fig. 2(b). The model points in Fig. 2(b) are those referred to in Fig. 6. Surface pressures were measured in a time-averaged manner using Sensym semiconductor transducers type LX-1620D operating in a differential mode as reported in more detail by Ashworth et al.[18]. Baseline experimental results have been reported by Ashworth et al. but for clarity some of this data is referred to in the present paper. The velocity triangle for the steady nominal design case is shown in Fig. 1(b) which includes the effect of the reduced NGV exit wake velocity C_2' on the rotor inlet angle β_1.

Experimental Results

Mean Heat Transfer Without Wake Interaction

A comparison of baseline data with no rotor/wake interaction is given in Fig. 3(a) for the two cases of low (< 0.8%) freestream turbulence and with a turbulence level of approximately 3%. It will be seen that the turbulence generated by the bar grid is sufficient to bring the region of boundary layer transition forward from about 60% x/s on the pressure surface and 50% x/s on the suction surface to 10% and 20% respectively. All of this data was taken at the nominal design cascade operating conditions:

$$T_{total} = 432\ K$$

$$M_{exit} = 1.18$$

(based on isentropic inlet total and pitchwise averaged exit static pressures)

$$Re = 0.919 \times 10^6$$

$$\beta_1 = 58.06°.$$

The circled numbers refer to heat transfer gauges identified in Fig. 2(a). The heat transfer rate is presented in terms of a non-dimensional Nusselt Number, defined as:

$$Nu = \frac{\dot{q}_{meas}}{(T_e - T_{meas})} \frac{C_t}{k}$$

Instantaneous and Mean Heat Transfer with Wake Interaction

The heat transfer rate to the blade with the additional effect of wake interaction is illustrated in Figs. 3(b) and 3(c) for both cases of effectively zero freestream urbulence and ~ 3% $u'/\bar{U}$. From Fig. 3(c) it will be seen that there is an overall increase in heat transfer rate over both the pressure and suction surfaces. The pressure surface heat transfer is enhanced over practically the whole length although the dominant effect is observed for values of x/s < 70%. On the pressure surface the effect of wake interaction persists to about x/s = 30%. Examples of instantaneous heat transfer rates are inset in the Figure and a more extensive 'atlas' of results is given in Ashworth et al.[18]. The heat transfer rates with wake interaction and with effectively zero freestream turbulence are shown in Fig. 3(b). As expected there is a marked increase in the level of heat transfer rate over almost the entire pressure

(a) Natural Transition of the Suction Surface Boundary Layer

Wide bandwidth heat transfer signals obtained from the surface thin film gauges clearly illustrate the important differences between the low and high freestream turbulence cases as shown in the high frequency traces of Fig. 6(a). There is a constant spacing of 5 mm between the thin film gauge results shown, starting with gauge 3 at an x/s value of 0.12 through to gauge 15 at x/s = 0.65. The low turbulence case (Run 5723) remains quiet (laminar) throughout the entire measuring range of the transient data (to x/s = 0.65). The surface heat transfer for the high freestream turbulence case, while starting somewhat higher than the laminar case, becomes increasingly dominated by sharp transient events (consistent with the theory of turbulent spot development, growth, and gradual merger as proposed by Emmons[20] and verified by many others (e.g. Schubauer and Klebanoff[21]). These spots, which raise the heat transfer coefficient instantaneously to high turbulent levels, continue to grow and merge until finally the Nusselt Number signals become increasingly characterised by the "steady" turbulent levels. It is clearly seen that by the x/s = 0.65 station the flow is at the turbulent level more than half of the time but drops precisely to the undisturbed laminar values between the turbulent events. In other tests conducted at 1.5 x Re design, the boundary layer was fully turbulent at this location.

The physical process of turbulent spot breakdown to turbulence can be seen in Fig. 6(a). The growth and rearward convection of individual turbulent spots is clearly seen as they move along the blade surface. The spot signals grow in height and width as the spots cover more of each succeeding thin film gauge and shift in time downstream. This breakdown process is quantified in more detail in Ashworth[22] where intermittency levels are estimated from the digital time records and spot convection rates are estimated from cross-correlation analysis of adjoining thin film signals.

(b) Detailed Wake and Shock Interaction Effects

It is possible to analyse the reaction of the blade boundary layer to the wake and shock perturbations with 2 bars rotating by investigation of the sequence of time-resolved Nusselt Number plots given in Fig. 6(b),(c) and (d). The high freestream turbulence case with wakes and shocks present (Fig. 6(b)) is markedly different to the naturally transitional boundary layer (Fig. 6(a)) over the first 35% of the surface, with similar rapid rises and falls in Nusselt Number to the perturbations evident in Fig. 5. This shock related event occurs on the early suction surface due to a shock/boundary layer interaction starting at gauge 9, close to the crown of the suction surface. Examination of the Schlieren photographs (Fig. 7) indicates that the shocks first interact with the boundary layer near to gauge 9, the reflection point moving towards the leading-edge as the bar moves in the same direction. This is visible on the early gauges on Fig. 6(b), occurring first on gauge 9 then moving gradually through gauges 7 and 5 and finally showing on gauge 3. The rapid drop in surface Nusselt Number is attributed to an unsteady separation and the rise to a turbulent re-attachment both caused by the shock boundary layer interaction. The effect of the wake is not clearly discernable in Fig. 6(b) and to aid in identification of this the bars were rotated at a lower speed such that the bar relative Mach Number was subsonic. The results of this are shown as Fig. 6(c) with a much more clearly identifiable enhancement in heat transfer due to this wake. This extends to the later gauges of the surface causing the boundary layer to be fully turbulent over the extent of the wake. In Fig. 6(d) the background turbulence was reduced to less than 0.8% and the periodic disturbances due to the bar-passing events are more clearly evident. The early suction surface has shock-related phenomena extending well into the cycle period with apparent oscillations in Nusselt Number moving with the shock. Also apparent from Fig. 6(d) is the intermittent nature of the turbulence induced in the boundary layer by the wake and shock interaction, as the boundary layer clearly returns to its undisturbed laminar value between the periodic events. The heat transfer enhancement due to the wake is clearly evident along the whole surface.

In summary, it appears that the state of the turbine boundary layer seems to be controlled by the level of freestream turbulence except in the region where the actual shock and wake passes through the cascade passage.

(i) A prediction of the flowfield velocity is made, in this case using the Denton scheme[34] and stored by the program.

(ii) U_{rel} is calculated (assumed constant across the span), the center-line of the undistorted wake is calculated from the specified bar position and the width added.

(iii) The wake is shifted back in time so that the bar will return to its correct position following the marching process of the prediction routine.

(iv) From this initial position elements of the wake are convected by small time steps using the local velocity interpolated from the prediction until the bar reaches the specified location. The differential velocities in the flowfield cause distortion of the wake along its length and across its width as it is accelerated through the passage.

This simple scheme, which could be incorporated in the blade design process, agrees well with the positions of the wake on the Schlieren photographs, so that the fraction of time that the heat transfer rate to the surface is affected by the wake could be calculated and included in the intermittency term of a prediction. It also demonstrates that to the level of our measuring ability second-order effects such as the "negative jet" effect do not significantly affect the wake position, as referred to in Doorly[33], and that the assumption that this flow unsteadiness may be superimposed on the steady flowfield is a valid approximation.

Quasi-3-Dimensional Shock Prediction

Although it was possible to model the wake in 2-dimensional terms, the shock structure associated with the transonic nature of the bar (as M_{rel} varies from 1.06 at the hub to 1.25 at the tip) is not strictly 2-dimensional, as has been seen in the Schlieren photographs (Fig. 7). An attempt was made to predict the positions of the bow and recompression shocks due to the bar in order to allow trajectory rate calculations to be made relating to the heat transfer measurements, and to aid in understanding phenomena observed in the Schlieren photographs. An example of such a prediction is presented as Fig. 9. The prediction is based on the assumption that for a small element of the bar the flow is 2-dimensional with respect to the plane containing U_{rel} and normal to the bar axis, a quasi-3-dimensional approach described in detail in Ashworth[35]. As U_{rel} varies in both magnitude and direction, so does the associated shock structure, and unlike the wake, this variation should be accounted for. The method of prediction was computerised as follows:

(i) For assumed constant inlet conditions and a specified position of the bar M_{rel} is calculated and its direction determined.

(ii) The equation of the bow shock in the 2-dimensional plane described above is derived from M_{rel} using the method described in Shapiro[36], shock properties and turning angles obtained by curve-fit equations where necessary over a range of Mach Number from 1.0 to 1.5.

(iii) The recompression shock is assumed to be straight and inclined at the Mach angle ($\sin^{-1} 1/M_{rel}$) to the direction of M_{rel}, with a virtual origin two diameters downstream of the bar.

(iv) The shocks are chopped and refracted if they are downstream of the blade axial leading-edge point, with allowance made for regeneration of the shock as it moves away from this point.

(v) Finally the points of intersection with the blade suction surface are calculated, and the shocks are simply reflected from an origin mid-way between the two intersection points.

Comparison with the Schlieren photographs is encouraging, the position shown in Fig. 9 corresponding to time 2 in Fig. 7., and it is hoped that information from this simplified model will prove useful as an aid to understanding the complex shock movements in turbine passages, in spite of the many simplifying assumptions made in this prediction (such as allowing for no variation of the freestream velocity).

Conclusions

It has been established during the course of this study that the Isentropic Light Piston Tunnel facility combined with the wide bandwidth/high sampling rate heat transfer instrumentation has proved capable of tracking very rapidly progressing unsteady events in a transonic boundary layer. Operating

14. Dring, R. P. and Joslyn, H. D., "The Relative Eddy in Axial Turbine Rotor Passages", ASME Paper No. 83-GT-22, 1983.

15. Dring, R. P., Joslyn, H. D., Hardin, L. W. and Wagner, J. H., "Turbine Rotor-Stator Interaction", ASME J. Eng. for Power, Vol. 104, pp. 729-742, 1982.

16. Epstein, A. H., Guenette, G. R. and Norton, R. J. G., "The MIT Blowdown Turbine Facility", ASME Paper No. 84-GT-116, 1984.

17. Schultz, D. L., Jones, T. V., Oldfield, M. L. G. and Daniels, L. C., "A New Transient Cascade Facility for the Measurement of Heat Transfer Rates", AGARD CP-229, 1977.

18. Ashworth, D. A., LaGraff, J. E., Schultz, D. L. and Grindrod, K. J., "Unsteady Aerodynamic and Heat Transfer Processes in a Transonic Turbine Stage", ASME Paper No. 85-GT-128, 1985.

19. Schultz, D. L. and Jones, T. V., "Heat Transfer Measurements in Short Duration Hypersonic Facilities", AGARDOGRAPH No. 165, 1973.

20. Emmons, H. W., "The Laminar-Turbulent Transition in a Boundary Layer - Part I", J. Aero. Sci., Vol. 18, No. 7, July, 1951.

21. Schubauer, G. B. and Klebanoff, P. S., "Contributions on the Mechanics of Boundary Layer Transition", NACA Report 1289, 1956.

22. Ashworth, D. A., LaGraff, J. E., and Schultz, D. L., "Unsteady Interaction Effects on a Transitional Turbine Blade Boundary Layer", Paper to be presented at the Joint ASME/JSME Gas Turbine Conference, March, 1987.

23. Doorly, D. J., "A Study of the Effect of Wake Passing on Turbine Blades", D.Phil. Thesis, University of Oxford, 1983.

24. Denton, J. D., "An Improved Time-Marching Method for Turbomachinery Flow Calculation", ASME J. Eng. for Power, Vol. 105, pp. 514-520, 1983.

25. Ashworth, D. A., "Unsteady Wake and Shock Interactions on a Transonic Turbine Blade", D.Phil. Thesis, University of Oxford, 1986.

26. Shapiro, A. S., "The Dynamics and Thermodynamics of Compressible Fluid Flow", Ronald Press, Vol. 2, pp. 884-886, 1954.

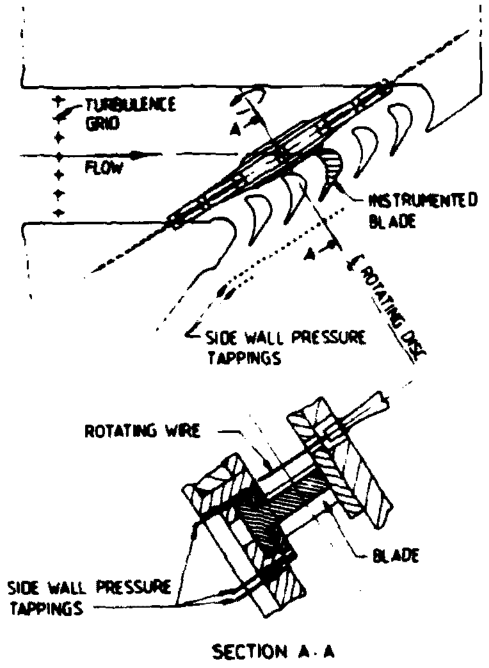

Fig. 1(a) Arrangement of the rotating bar wake generator and cascade.

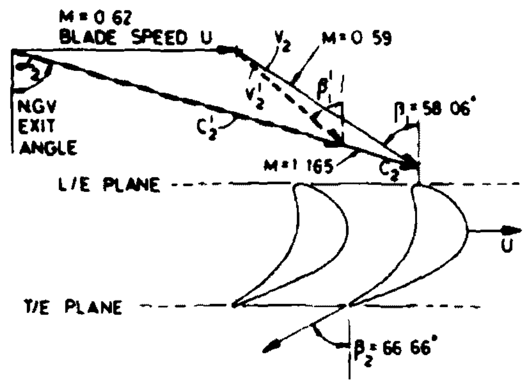

Fig. 1(b) Velocity triangles at inlet for the steady nominal design case at mid-span, showing the reduced incidence caused by the deficit in the wake.

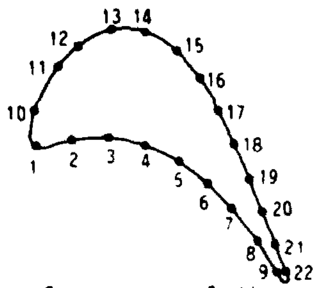

Pressure Surface

Model Point	x/s
1	0.00
2	0.12
3	0.24
4	0.36
5	0.48
6	0.59
7	0.71
8	0.84
9	0.96

Suction Surface

Model Point	x/s
10	0.08
11	0.18
12	0.24
13	0.31
14	0.38
15	0.46
16	0.53
17	0.61
18	0.68
19	0.76
20	0.83
21	0.90
22	0.96

(a)

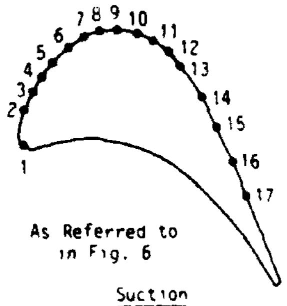

Suction Surface

Model Point	x/s
1	0.00
2	0.08
3	0.12
4	0.15
5	0.19
6	0.24
7	0.28
8	0.31
9	0.35
10	0 39
11	0.43
12	0.47
13	0.51
14	0.58
15	0.65
16	0.73
17	0.81

(b)

Fig. 2(a) Co-ordinates of the original heat transfer gauges on the blade profile.

Fig. 2(b) Co-ordinates of the heat transfer gauges for the detailed suction surface study, referred to in Fig. 6.

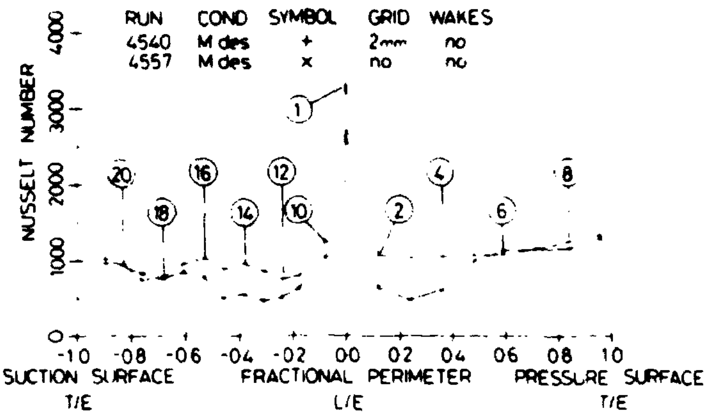

Fig. 3(a) Effect of freestream turbulence level on mean heat transfer rate without wakes for the nominal design case, M_2 = 1.18, Re = 0.919E6.

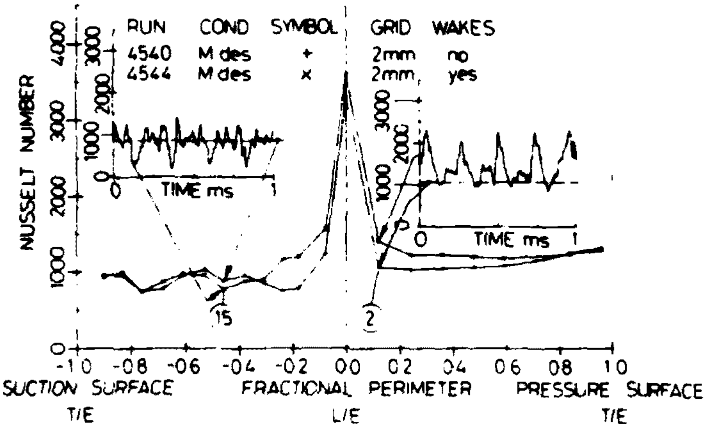

Fig. 3(b) Effect of wake and shock interaction on mean heat transfer rate at the high free-stream turbulence case (~ 3%) and design operating conditions. Inset are typical transient recorder signals for the 16 bar experiment at two x/s locations showing a 1 ms interval of the record together with the time-averaged values without the wake and shock interactions.

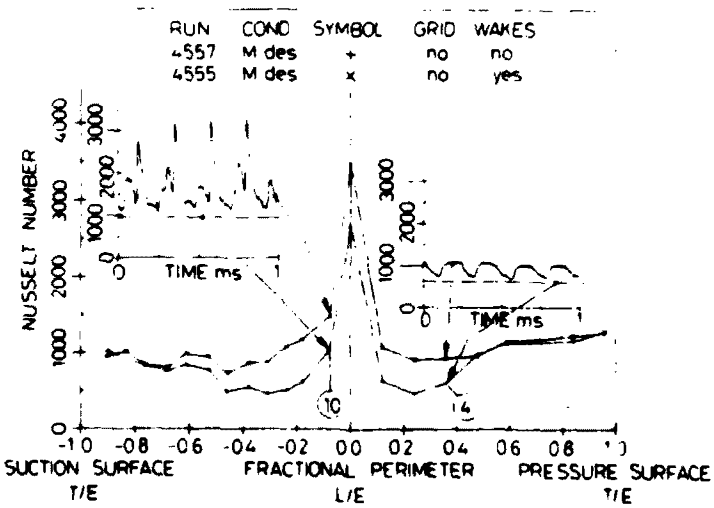

Fig. 3(c) Effect of wake and shock interaction on mean heat transfer rate for the low free-stream turbulence case (< .8%), otherwise as in Fig. 3(b).

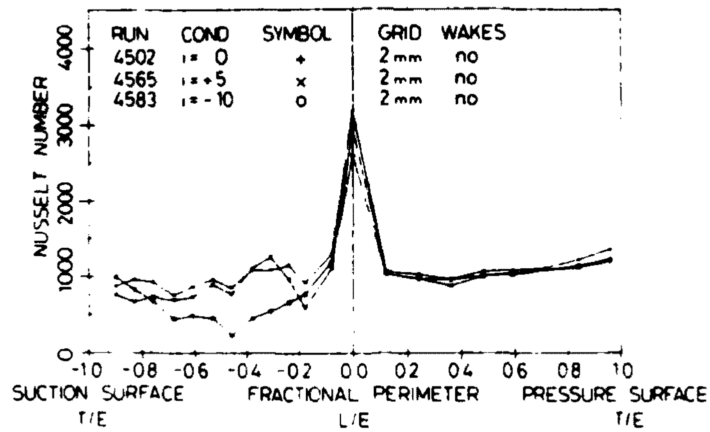

Fig. 4(a) Effect of incidence variation on mean heat transfer rate at the nominal design case (M_2 = 1.18, Re = 0.919E6) with no wake and shock interaction.

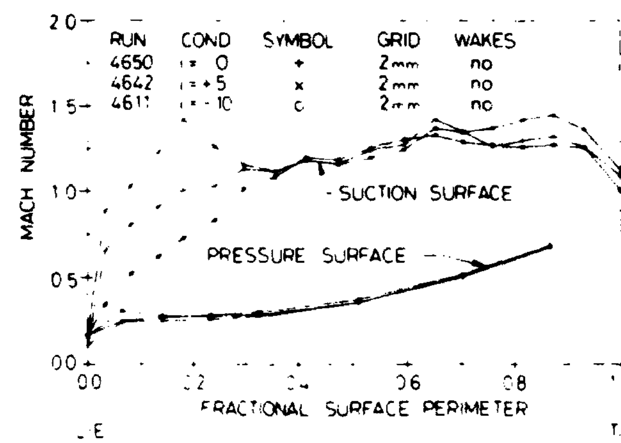

Fig. 4(b) Effect of incidence variation on mean surface isentropic Mach Number at the nominal design case (M_2 = 1.18, Re = 0.919E6).

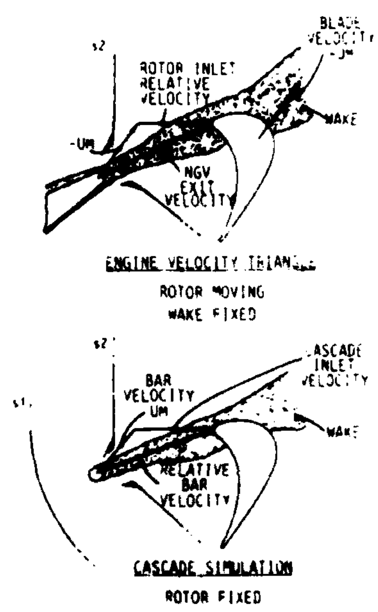

Fig. 5(a) Illustration of the comparative velocity triangles for the engine and cascade simulation of the NGV/rotor interaction.

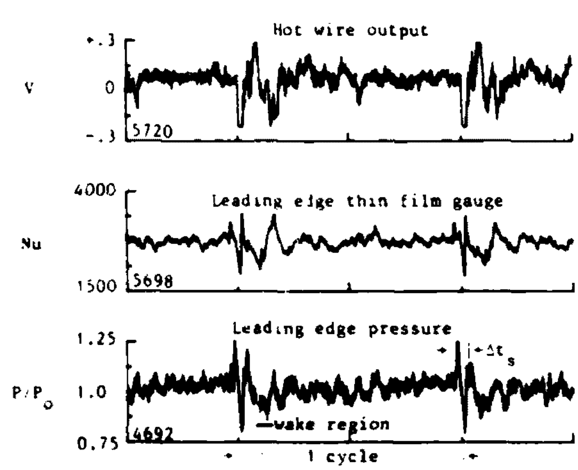

Fig. 5(b) Measurements of the unsteady disturbance at inlet by a hot-wire in the freestream and heat transfer and pressure measurements at the stagnation point.

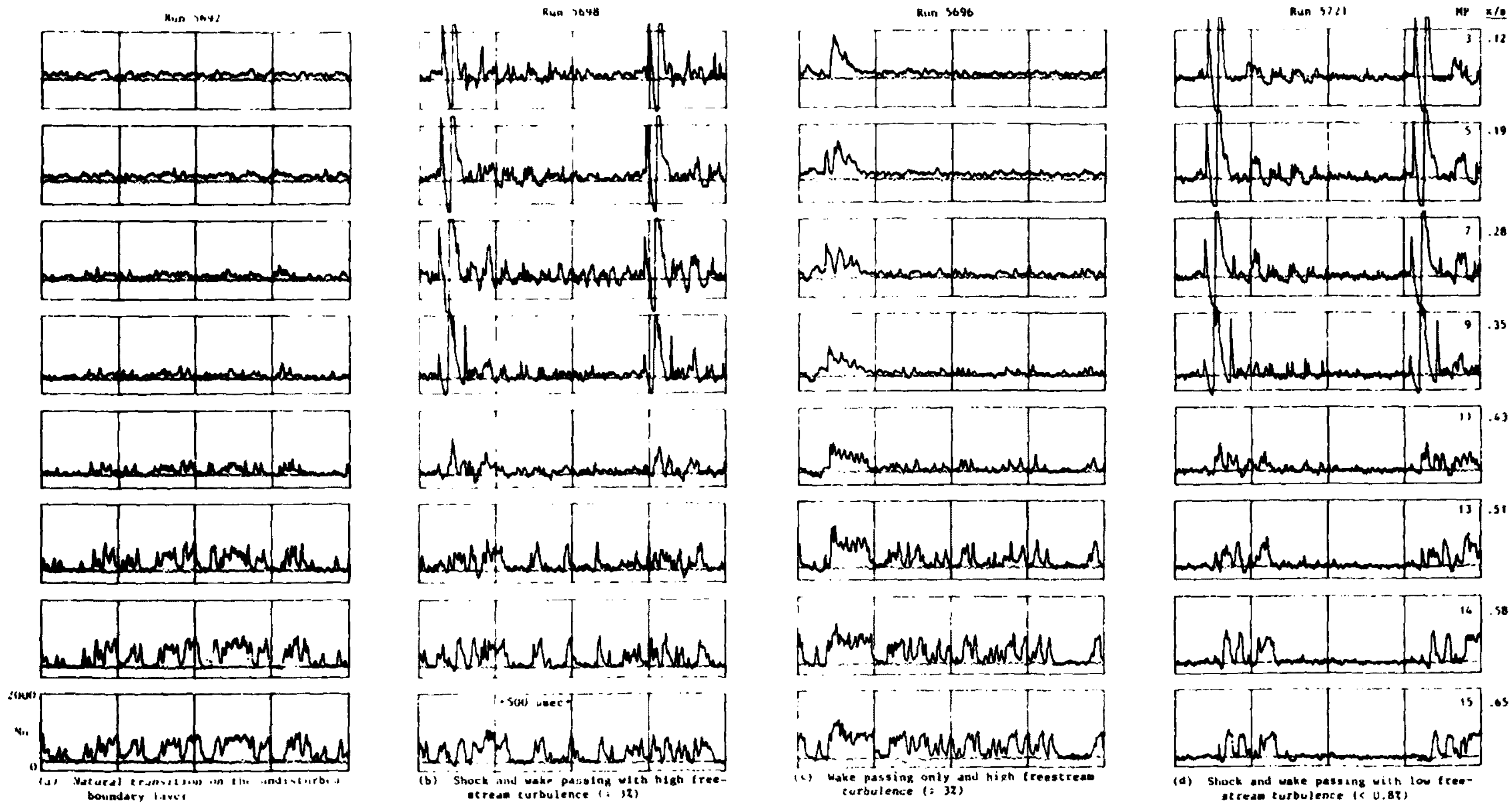

Fig. 6 Detailed time-resolved heat transfer rate measurements to the blade suction surface. The dotted lines are the baseline undisturbed results for the low freestream turbulence case (< 1%, Run 5723).

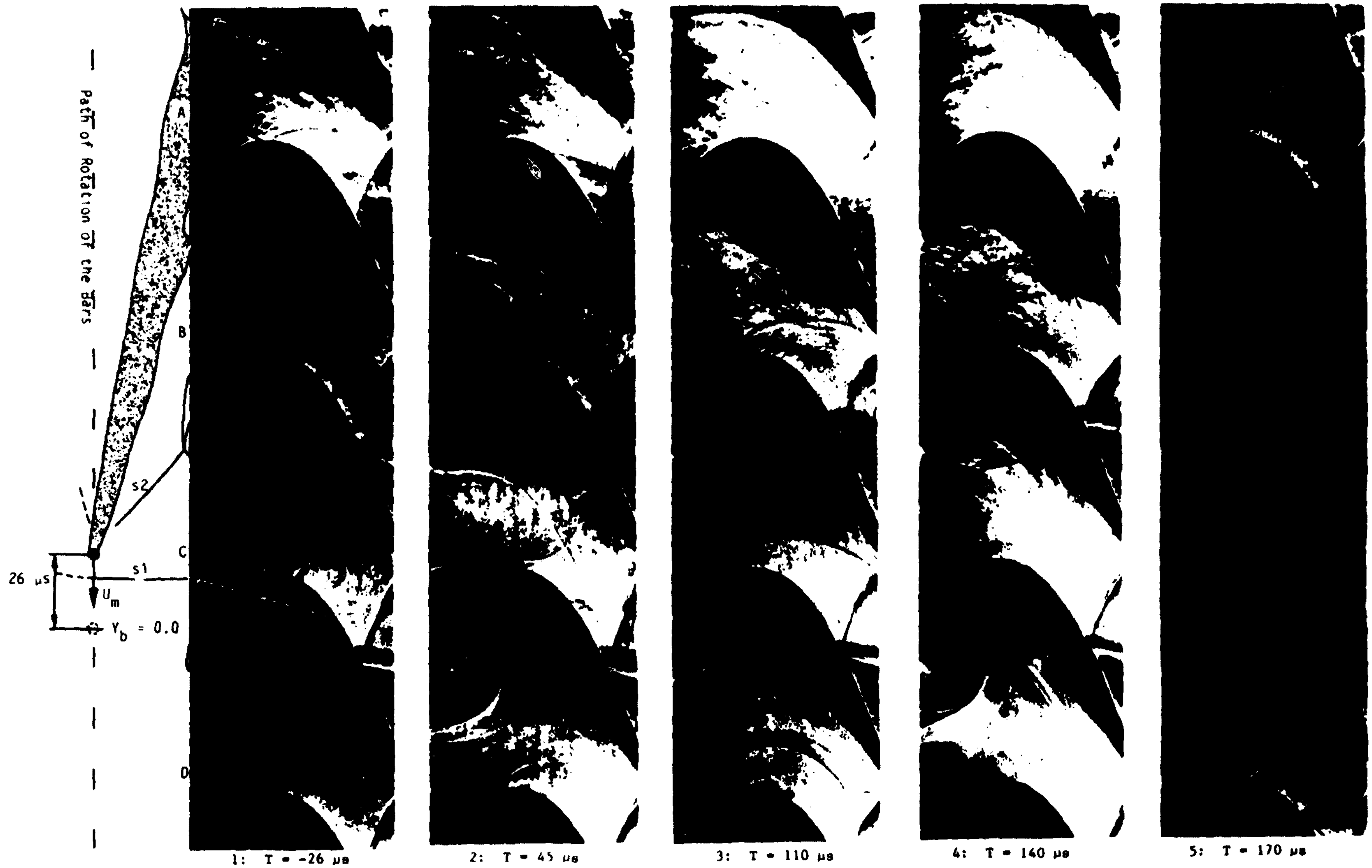

Fig. 7 Schlieren photographs of the cascade for different times in the bar-passing cycle. The position of the bar corresponding to time 1, the left-hand photograph, is illustrated with a sketch of the expected wake and shock positions (not visible in the photographs due to the limits of the Schlieren window).

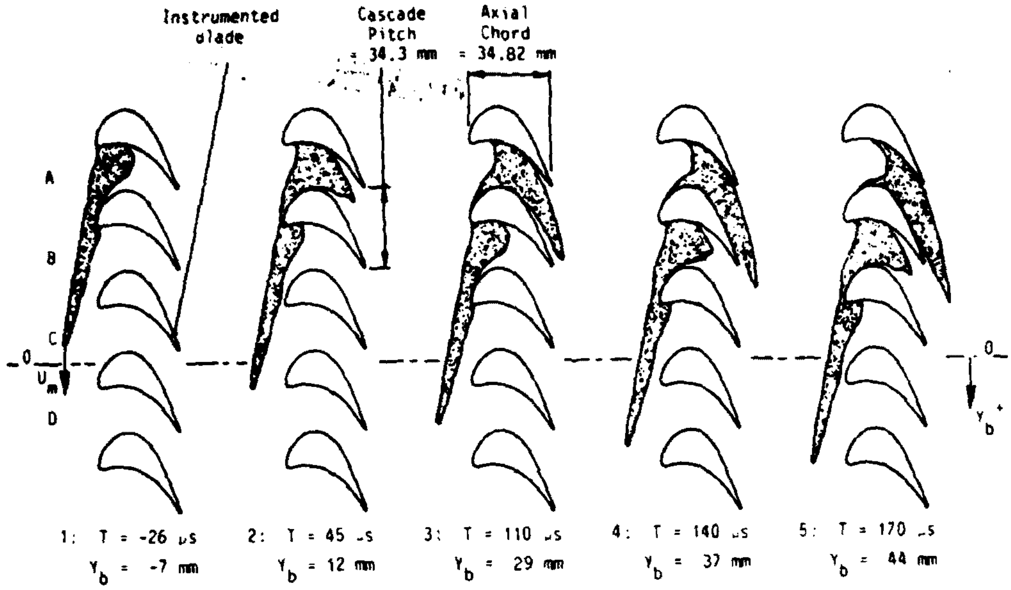

Fig. 8 Predicted wake positions at times corresponding to the Schlieren photographs in Fig. 7. The two lines for each time are the leading and trailing edges of the highly turbulent wake region.

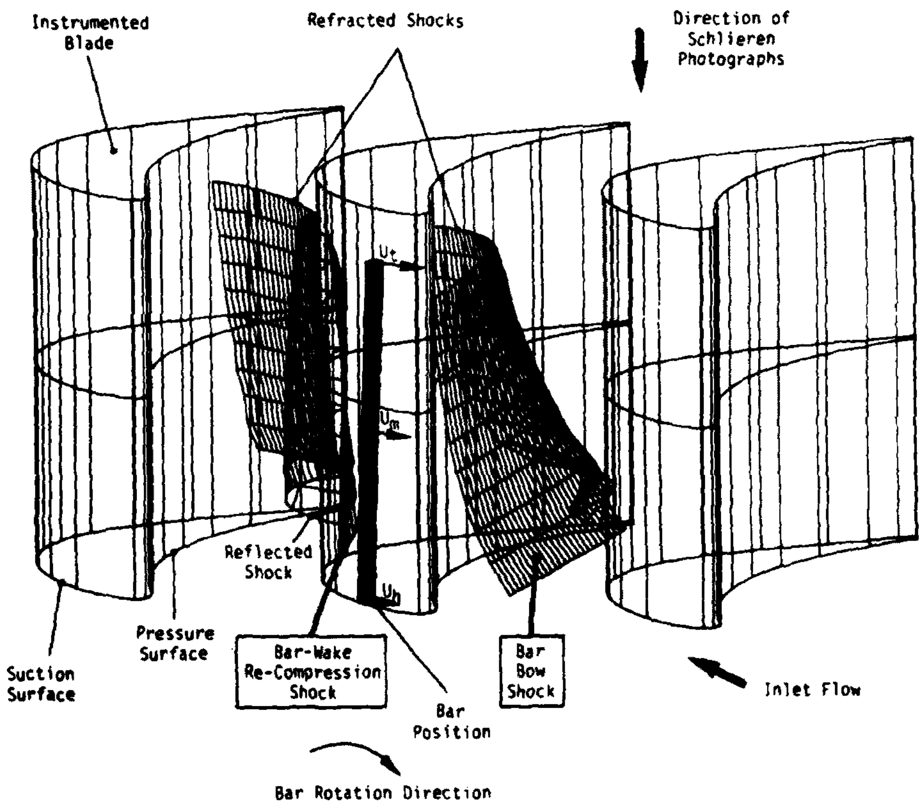

Fig. 9 Predicted shock position corresponding to time 2 of Fig. 7, with the bar inclined at ~ 2° to its datum position. Only the half of the shocks downstream of the bar are shown for clarity. The refraction and reflection of both shocks can be seen, with the re-compression shock more 2-dimensional in form than the detached bow shock, due to stand-off distance variation with bar relative Mach Number. Both shocks are weaker towards the hub due to the lower Mach Number there, with the bow shock strength less than the re-compression shock strength at each radius.

END

DATE FILMED

3-87

DTIC